Active thermal dissipation of semiconductor lasers for application in telecommunications

Mariana Marques Cardoso

Thesis to obtain the Master Science Degree in

Electrical and Computer Engineering

Supervisors: Prof. Paulo Sérgio de Brito André

Eng. Carlo Marques

Examination Committee:

Chairperson: Prof. José Eduardo Charters Ribeiro da Cunha Sanguino

Supervisor: Prof. Paulo Sérgio de Brito André

Members of the Committee: Prof. Horácio João Matos Fernandes

May 2017

ACKNOWLEDGMENTS

I would like to thank everyone who has helped me through the completion of this dissertation. Firstly, I express my sincere gratitude to the wonderful mentor Prof. Paulo Sérgio de Brito André for selecting me for this dissertation. His guidance, support and knowledge have been especially invaluable to me. This work would not have been possible without his limitless encouragement and insight.

I would also like to thank *Coriant* for providing me with a working space in their facilities in Lisbon. I especially am grateful for the guidance provided by my co-supervisor Eng. Carlo Marques who has lent his knowledge, time and expertise while designing the experimental setup and was essential for me to understand the importance of this thesis.

Finally a special thanks to my friends, to my boyfriend and to my family, particularly my sister and my parents, for all the love and endless support.

RESUMO

O laser semicondutor é um elemento vital na implementação dos sistemas de comunicações óticas. A crescente necessidade de largura de banda impulsionou o crescimento das redes de fibra ótica e a procura por mais funcionalidades levou ao aumento das densidades térmicas nos encapsulamentos dos lasers semicondutores. Devido à grande dependência do desempenho do laser semicondutor às variações de temperatura, o elemento de *peltier* presente no encapsulamento tem que ser capaz de remover o calor gerado de forma a obter uma temperatura de funcionamento estável.

O único método para avaliar o desempenho de um elemento é através da análise do modelo analítico do sistema usando propriedades dos materiais que muitas das vezes não são fornecidas pelos fabricantes. Este trabalho estuda a abordagem para a obtenção destes parâmetros através de uma ferramenta de minimização. A contribuição final desta tese é o desenvolvimento de um simulador do modelo térmico com parâmetros ajustáveis para um laser semicondutor com controlador de temperatura.

Palavras-chave — Comunicações óticas, TEC, laser semicondutor

ABSTRACT

The semiconductor laser is vital in the implementation of optical communications systems. The increasing demand for bandwidth has resulted in the growth of fiber optic-based networks and the rising demands for more functionality has lead to increased packaging and thermal power densities. Due to the heavy dependency of the semiconductor laser's performance to the temperature, the thermoelectric cooler must be capable of removing the generated heat to obtain a controlled functioning temperature.

The only method to evaluate the performance of a product would be through analytical modeling using material properties that are usually undisclosed by the manufactures. This work studies the approach of obtaining such parameters through a minimization tool. The final contribution of this thesis is the development of a simulator of a thermal model for a temperature controlled semiconductor laser with tunable parameters.

Keywords — Optical Communications, TEC, semiconductor laser

CONTENTS

LIST OF FIGURES

LIST OF TABLES

NOMENCLATURE

k	Boltzmann constant
T	Temperature
N_1	Atoms population at ground state
N_2	Atoms population at an excited level
L	Distance between the cavity mirrors
n	harmonic mode of the wave
λ_p	peak wavelength
$\Delta\lambda$	spectral width
$\delta\lambda$	spacing between longitudinal modes
J_{th}	threshold current density
r_e	extinction ratio
P_1	logical power level “1”
P_0	logical power level “0”
α	Seebeck coefficient
Q	rate of heat transfer
π	Peltier coefficient
τ	Thomson coefficient

I_{th}	threshold current
c_p	specific heat at constant pressure
c_v	specific heat at constant volume
q_c	Convective heat flow rate from the surface
h_c	Coefficient of convective heat transfer
A_s	Surface area for heat transfer
T_s	Surface temperature
T_m	Coolant media temperature
q_r	Heat transferred by radiation
ϵ	Emissivity of the radiating surface
σ	Stefan-Boltzmann constant
$F_{1,2}$	Shape factor between surface area of body 1 and 2
K	Thermal conductivity
$\vec{J}$	constant current flux
ρ_m	mass density of the material
$\dot{q}$	heat generated per unit volume
c_m	mass specific heat capacity
C	heat capacity
R	Electrical resistance

I_p	Peltier current
P_l	Optical power of the laser
t_1	Exponential time constant 1
t_2	Exponential time constant 2

GLOSSARY

CC	Constant Current
CV	Constant Voltage
DC	Direct Current
DFB	Distributed Feedback
DWDM	Dense Wavelength Division Multiplexing
FBG	Fiber Bragg Grating
LD	Laser Diode
MQW	Multi Quantum Wells
NMSE	Normalized Mean Square Error
NTC	Negative Temperature Coefficient
TEC	Thermoelectric Cooler

1. INTRODUCTION

1.1. MOTIVATION

The importance to transmit information quickly, correctly, and efficiently has always been one of the main focuses driving human innovation [1]. Man's first attempts to communicate remotely were limited with the use of beacon fires, smoke signals and signal markers [2]. With the invention of laser in 1960 by Theodore Maiman [3] and the laser diode two years later by Robert Hall [4], [5], two of the most significant breakthroughs for human technology in the last century, optical communications were allowed to evolve to what we know today.

The laser diode or semiconductor laser has quickly become vital in the modern world due to its importance in the implementation of optical communications systems. A major benefit to light communications is the multiple mediums of information transport as laser light can be transmitted by direct line of sight or by means of a fiber optics cable. Additionally, multiple signals along a single pathway can be achieved with high quality and low losses. These advantages make semiconductor lasers the standard for the current telecommunications industry, which demands these properties for high speed data transmission [6].

The increasing number of applications becoming online at every second, the explosion of the smartphone and tablet use and the resulting growth of the wireless stream of high definition video and games are placing a huge strain in today's networks design. This continued demand for increased bandwidth has resulted in the growth of fiber optic-based networks. Today virtually the entire undersea and land-based long-haul communication network is optical [7]. Submarine data cables handle more than 95 percent of IP voice and data traffic between countries and continents, and 100 percent of international Internet traffic [7]. According to Cisco Visual Networking Index, the annual global IP traffic will reach 2.3 ZB by 2020. IP traffic will grow at a compound annual growth rate of 22 percent from 2015 to 2020 [8]. To follow these rapid changes, equipment manufacturers and designers need to evolve and expand at a high rate and scale and at low cost to enable the next many generations of efficient and scalable telecommunications products. The level of integration required has severe implications for hardware design in general but even more considerable challenges from a thermal perspective. Packing so much functionality devices and components into smaller package will lead to substantially increased thermal densities which in turn will require deployment of new thermal solutions [9].

Concerns over the environment and energy consumption have placed an emphasis on the development of new more efficient and less pollutant technologies and an improvement of the efficiency in optical transmission [9]. Improved network element efficiency partly comes from improvements in the underlying optical and electronic components, and how they are employed. Optical fiber-based amplifiers are perhaps approaching the peak of their performance potential, but would benefit from more efficient pump lasers [10], [11]. Within the central office or data centre, the overall savings of energy through improved power efficiency of the individual component parts is multiplied up by the so called “energy escalator”. The telecom operator Verizon has estimated that each watt saved on an equipment card is multiplied by 2.41 when the impact of air-conditioning and cascaded power converter inefficiencies in the central office is taken into account [12]. For many optical devices, this is because it is necessary to use localized thermoelectric coolers within the component.

Laser lifetime and operational efficiency suffer severely with increasing temperature. If the laser diodes operating temperature is reduced by 10°C, the lifetime could statistically double [13], [14]. Additionally, the necessity for the devices to be small prevents conventional cooling from being useful. Temperature does not only influence the efficiency of the laser diode, but the wavelength of the laser as well, due to the fact that pronounced temperature changes in the diode can cause shift in the emission wavelength. The narrow channel spacing in WDM systems relies on laser wavelength being controlled within the sub-nanometer scale. Due to the ambient temperature variation and laser operation uncertainties, the temperature controller must be capable of removing heat to maintain control. It requires a precision temperature controller capable of maintaining control well inside 0.1°C over time and temperature variations [15]. Thermoelectric coolers (TEC) being reliable, compact and quiet, allow this.

While these devices contribute for a good laser performance, they can consume and dissipate twice as much power as they remove [16]. Consequently, for these widely used and necessary temperature controlled DWDM lasers each watt of power consumed by the laser transmitter can result in up to 6 watts of power taken from the grid [17]. If the absolute conversion efficiency of electricity into photons is also considered the situation would appear even worse with 1W of optical power transmitted out of the central office requiring up to nearly 1kW of electrical power from the grid [17]. However, as most of the power in today’s central office is consumed by the electronics and not the optics, this has not been considered previously to be so significant. But with the projected need for Terabit inter-connectivity, optics will increasingly play a greater role, and in particular, the use of dense and ultra-dense WDM with spectrally efficient transmission formats will become widespread. These advanced transmission formats will actually consume more electrical power per bit unless urgent attention is paid to better understand and efficiently use these devices.

1.2. STATE OF THE ART

The discovery of the thermoelectric effect began in 1821 when the German physicist Thomas Johann Seebeck, discovered that a potential difference was produced in a circuit of two dissimilar metals when one of the junctions of circuit was heated or at a higher temperature than the other junction [18]. He named this phenomenon "*the magnetic polarization of metals and ores produced by a temperature difference*" and, not realizing that he had found out a new source of electric current, claimed this was due to magnetism induced by the temperature difference and thought it might been related to the Earth's magnetic field. However, it was later realized that a "Thermoelectric Force" induced an electrical current, which by Ampere's law deflects the magnet. More specifically, the temperature difference produces an electric potential (voltage) which can drive an electric current in a closed circuit. Today, this is known as the *Seebeck* effect.

In 1834, shortly after the discovery of the Seebeck effect, Jean C. A. Peltier discovered the reverse phenomenon, the *Peltier* effect [19]. He observed that by passing a current through a junction of two dissimilar metals, a temperature gradient could be produced in the metal junction. The direction of current would determine the direction of heating or cooling. When the current passed in one direction there was a cooling effect at one end. When the current direction changed, the cooling occurred at the opposite end. This discovery was later reinforced in 1838 when E. Lenz proved that the Peltier effect was an autonomous physical phenomenon, which consisted in releasing and absorbing of additional heat on conductor's junctions when current passed through them and that depended on current direction [20]. He concluded that, depending upon the direction of the current flow, heat is absorbed or generated at a junction between two conductors and demonstrated this by freezing water at a bismuth-junction and melting the ice by reversing the direction of current flow.

The *Seebeck* effect and the *Peltier* effect were finally mathematically derived by the English physicist William Thomson, later referred to as Lord Kelvin [21]. By using thermodynamic arguments he unified the *Seebeck* and *Peltier* effects into one single expression giving decisive arguments in favor of a complete and compact description of all these phenomena. With this theoretical analysis of the relationship between both effects he was able to show that a third effect has to exist. This third effect bearing his name is the absorption or emission of heat along a current carrying conductor with a temperature gradient, such as a wire with current passing through it, depending on the material of the conductor and the direction of the current. These three closely related effects cumulatively give rise to the thermoelectric phenomenon as a whole and can be exploited to produce power and refrigeration. These effects are not exclusive to thermoelectric materials alone but are present in all metals and semi-metals. Only in select

combinations of dissimilar semi-metals (thermoelectric materials) are their effects most observable and practical from an application standpoint.

Even though the thermoelectric coolers fundamentals were already known, early efforts showed only negligible benefits due to material limitations. In 1911 was demonstrated that a good thermoelectric material would have a high Seebeck coefficient, a high electrical conductivity and a low thermal conductivity [22]. Only after the semiconductors started becoming mass-produced in the 1950s for transistor manufacturing did the importance of thermoelectrics become evident. After the semiconductor materials became more widespread their thermoelectric properties were explored.

In the late 1960s IBM expressed interest in thermoelectric cooling applications which included cooling an infrared diode, a temperature controlled enclosure, a thermoelectric heat exchanger for use in a thermal control system for wafer testing, and a thermoelectric wafer cooling platform. In 1967, IBM began to investigate the application of thermoelectric cooler modules to cool an optical diode employed in a computer communication data link. [23] The schematic of the developed system is seen in Figure 1.1.

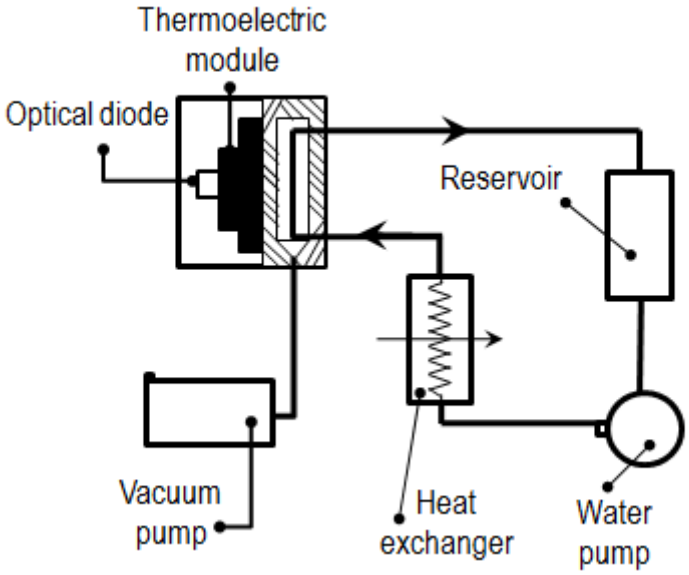

Figure 1.1 Schematic of a thermoelectric cooling system for an optical data link

This solution included an optical diode emitting light in the infrared range and had the potential of removing 3 Watts of heat that was essential to the operation of the link. To make sure the process had a consistent operation, the optical diode was mounted on a two-stage cascaded thermoelectric cooler with the cold side surface temperature at -25ºC and the hot side temperature at 55ºC. A secondary source of heat removal is crucial for the thermoelectric cooler to operate so in this system an indirect cooling method, or water-cooled loop, was implemented to remove the heat from the thermoelectric cooler and radiate it to the exterior. The

thermoelectric cooler and the optical diode were mounted in a chamber with a small vacuum pump operated continuously to counteract any moisture buildup and water vapor condensation on the surfaces of the thermoelectric device. The light signal was then collected from the optical diode from a window in the sealed chamber. The viability of this solution was achieved due to the fact that the thermoelectric cooler devices are small and ensured the control necessities required by the optical diode.

In 1990, trends in laser packaging already dictated the need for thermoelectric coolers and included them in their laser packaging [24]. This second generation system employed a modern method that draw the heat from the laser diode and expedite it through an efficient heat sink to air. For high data-rate packages, the need for a good control of the laser's temperature was becoming a necessity due to the temperature dependent laser characteristics combined with systems designers demanding wider temperature operating ranges and more efficient TECs.

This second generation system was more modern and devices draw the heat from the laser diode and expedite it through a heat sink to air. For high data-rate packages, the need for a good control of the laser's temperature was becoming very evident because of the temperature dependent laser characteristics and systems designers were demanding wider temperature operating ranges and more efficient TECs.

1.3. THESIS OBJECTIVES

The main objective of this thesis is to develop a thermal model for a semiconductor laser. Other objective is the optimization of its thermal management through an efficient use of the thermoelectric cooler characteristics whilst reducing the power consumption. Understanding the thermal model and finding the real parameters that describe the energy exchange inside the laser packaging allows not only a more capable temperature controller but also provides valuable information to the designer that struggles to build more functionality into a shrinking package space. Laser packaging systems require an efficient thermal operation provided through the smallest solution size to avoid excessive heat dissipation through unnecessary bulky passive heat sinks. By acknowledging the real parameters of the system the packaging can be designed in the best efficient way. Therefore a method to extract the thermal parameters from a laser was developed.

Part of the experimental procedures described in this thesis took place in *Coriant*'s facilities in Alfragide, namely the parameter assessment of the laser diode with thermoelectric cooler. The objective was to describe the system to then optimize the energy consumption of the optical communication's boards.

Chapter 2 provides the theory of the semiconductor laser and the fundamentals of its operation to reinforce and justify the need for the thermal management inside their packaging. It also provides the theory behind the thermal management techniques and the thermal characterization of the system laser diode and its peltier cooler.

Chapter 3 presents the thermal model developed for both the peltier module and the system laser and its thermoelectric cooler. It provides all the simplifications and assumptions considered in this thesis and the equations that will be subsequently used to determine the values of the unknown parameters that describe the system. Finally it is described the simulator created for the thermal model.

In chapter 4 will be verified the need for an efficient laser temperature control through an experiment that will measure in laboratorial conditions the effect of the temperature on the performance of the semiconductor laser.

Chapter 5 describes the procedures used for the extraction of the parameters that describe the peltier module. It also provides the results after the minimization for the system.

In chapter 6 the laser semiconductor is introduced to the system and like in the previous chapter the procedures for the extraction of the parameters that describe this new system will be presented. It's also presented the effect of the ambient temperature, heat sink solution and the laser's power variances on the temperatures of the system.

In chapter 7 the final conclusions of this work and suggestions for future improvements on this topic are presented.

2. THEORETICAL BACKGROUND

2.1. FUNDAMENTALS OF LASER OPERATION

To realize the importance of controlling the laser's thermal stability is necessary to understand the fundamentals and basic principles of lasers and conditions necessary for a good quality diode laser operation.

The word LASER is an acronym for Light *Amplification by Stimulated Emission of Radiation.* Stimulated emission of radiation is a natural process first identified by Einstein. It occurs when a beam of light passes through a specially prepared medium and initiates or stimulates the atoms within that medium to emit light in exactly the same direction and exactly at the same wavelength as that of the original beam. A typical laser device (Figure 2.1) consists of an amplifying or gain medium, a pumping source to input energy into the device, and an optical cavity or mirror arrangement that reflects the beam of light back and forth through the gain medium for further amplification. A useful laser beam is obtained by allowing a small portion of the light to escape by passing through one of the mirrors that is partially transmitting.

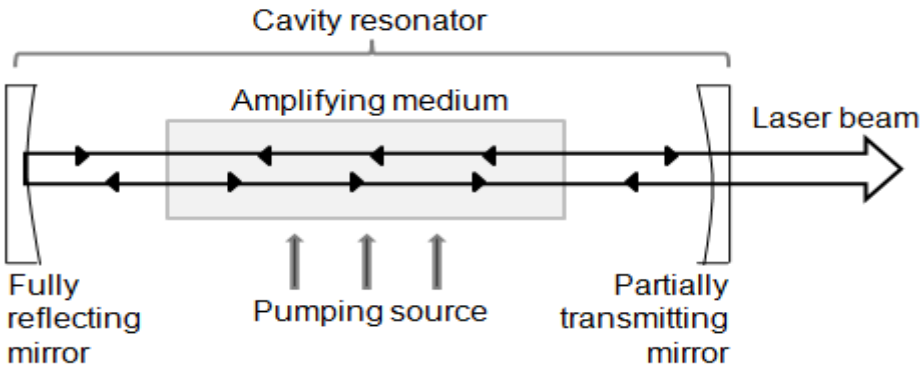

Figure 2.1 Basic laser components

When an atom is excited to a high-energy state, it can lose that energy and fall to a lower-energy state producing a particle of visible light or photon.

Any electron in an atom or molecule has its own stable states in which the atom has a specific energy level. When there's enough energy injected into an atom, the electron acquires the energy and by doing that it makes a transition from one stationary state to another, entering an excited state. From that excited state the electron can lose energy and fall to a lower-energy

state, but due to the principle of conservation of energy, the difference in energy between the initial high-energy state and the final low-energy state appears either as a photon of emitted light, as energy transferred to another state or atom or as heat. [25]

The transition frequency between two energy levels f is related to the energies of the two states so the wavelength of the emitted photon can be predicted by Planck's relationship

$$E_{photon} = E_2 - E_1 = hf \tag{2.1}$$

where E_1 and E_2 are energy levels of the low and high-energy state in an atom or molecule and h is Planck's constant.

There are three different kinds of atomic transitions between two different states due to the interaction of light. The first type of transition of an atom is referred to as absorption. When an atom is residing at a low-energy state with energy E_1 it can absorb enough energy so that it will transfer to a higher-energy state. The energy absorbed can be in different forms, including electrical, thermal, optical, chemical, or nuclear. Initially the atom stays in the ground state until a photon of with energy larger than the difference between the two atomic energy states is incident. In this situation the atom will transit from the ground state E_1 to the higher level E_2 by absorption of the incident photon.

Regardless of the excitation method, an atom in a high-energy state will eventually fall to a lower-energy state since nature favors a lower-energy state. In jumping from a high to a low-energy state, a photon will be produced, with the photon energy being the difference in energy between the two atomic energy states. Since each atom makes a transition independently, a photon is emitted in a random direction with a random phase and frequency. Such light is incoherent and the process is designed as spontaneous emission.

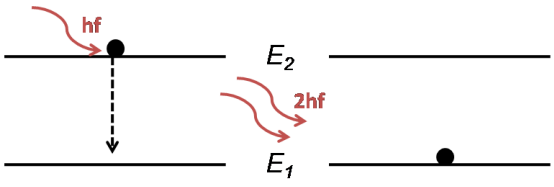

Figure 2.2 Energy level representation of stimulated emission before (left) and after (right)

The third kind of atomic transition described in Figure 2.2 is referred to as stimulated emission. In this case, an atom is initially in the high-energy state, and a photon with energy higher than the difference between the high and low-energy states is incident on it. The incident photon will cause the atom to undergo a transition from E_2 to E_1 emitting a stimulated photon whose properties are identical to those of the incident photon in addition to the incident photon. The fact that the generated photon has the same wavelength, phase and direction as that of an

incident photon makes the emitted radiation coherent and monochromatic, two key properties of laser light. The fact that these two photons are emitted in the same direction will be essential to making the light collimated, the third key property of laser light.

In order to generate the desirable coherent light, atoms or molecules must make transitions by stimulated emission. To do so, more atoms must be in a higher excited state than in lower energy levels. This condition is essential so as to the light emitted by stimulated emissions won't be re-absorbed by atoms at a rate that is superior to the emission rate.

Thermal energy is present in every system and excites atoms raising them to higher energy levels so that the more thermal energy that is injected into a system, the more higher-energy levels will be populated. The resulting distribution of energy, describing the population of atoms at each energy level, is governed by Boltzmann's law, one of the fundamental laws of thermodynamics. Boltzmann's law predicts the population of atoms allowing us to predict the distribution of atoms at any given energy level:

$$\frac{N_2}{N_1} = \exp\left(-\frac{\Delta E}{kT}\right) \tag{2.2}$$

where N_2 is the population of atoms at an excited energy level, N_1 the population of atoms at ground state, ΔE the energy difference between the two states in Joules, k is Boltzmann's constant, and T is the absolute temperature in Kelvin.

When there is no external source of energy a system is at thermal equilibrium. This means that the quantity of atoms at a certain energy level depends only to the present temperature.

By inspecting equation (2.2) we can verify that even if the temperature of the entire system were to be raised and the distribution shifted so that more atoms would reach higher energies, the population of the ground lower-energy level would still always beat that of a higher-energy level.

In order to generate a lasing action, atoms or molecules must make transitions by stimulated emission. Do to so, energy is injected into a system at thermal equilibrium so that there are more atoms in a higher excited state than in lower energy levels ($N_2 > N_1$). Such a nonequilibrium condition is required for lasing action where the light emitted by stimulated emissions surpass the re-absorption. Therefore, external pumping of atoms to higher states is essential to accomplish population inversion.

Pumping is the process of supplying energy to the laser medium to excite the upper energy levels. It may be accomplished by any number of means, including electrical, thermal, optical, chemical, or nuclear. Most common lasers utilize electrical pumping or optical pumping.

An optical resonator is necessary in lasers to enhance the circulating power and it is used to feedback generated coherent light into the medium to the point where gain exceeds losses and increases the rate of stimulated emission.

The coherent light of a laser is achieved by coupling the medium with a laser cavity. The cavity is resonant at wavelengths such that the number of waves inside the cavity is an integer, the standing waves inside the cavity. For all other wavelengths, destructive interference causes these to be extinguished. These resonant wavelengths are called longitudinal modes and are spaced apart at regular intervals of frequency.

The condition for a standing wave in the cavity is

$$\lambda_n = 2L/m \tag{2.3}$$

where L is the distance between the cavity mirrors and m is the harmonic mode of the wave. This limits the wavelength and direction of the photons allowed to re-propagate through the medium. These photons provoke other photons with the same characteristics via stimulated emission so that all the photons propagating through the cavity are coherent. The rate at which the photons increase other photons via stimulated emission is called gain. To have a functioning laser it is essential that losses be kept to a minimum. The output transmission of the laser depends on its gain. When total losses in the laser exceed the gain of the medium, the laser will fail to oscillate so it's important to reduce the losses in the cavity so that the power output may be improved.

As previously said, semiconductor lasers emit light through stimulated emission. As a result of the fundamental differences between spontaneous and stimulated emission, they are not only capable of emitting high powers, but also have other advantages related to the coherent nature of emitted light. A semiconductor laser is pumped by electric current and its basic structure is a p-n junction. For this reason, semiconductor laser is also called injection laser or diode laser.

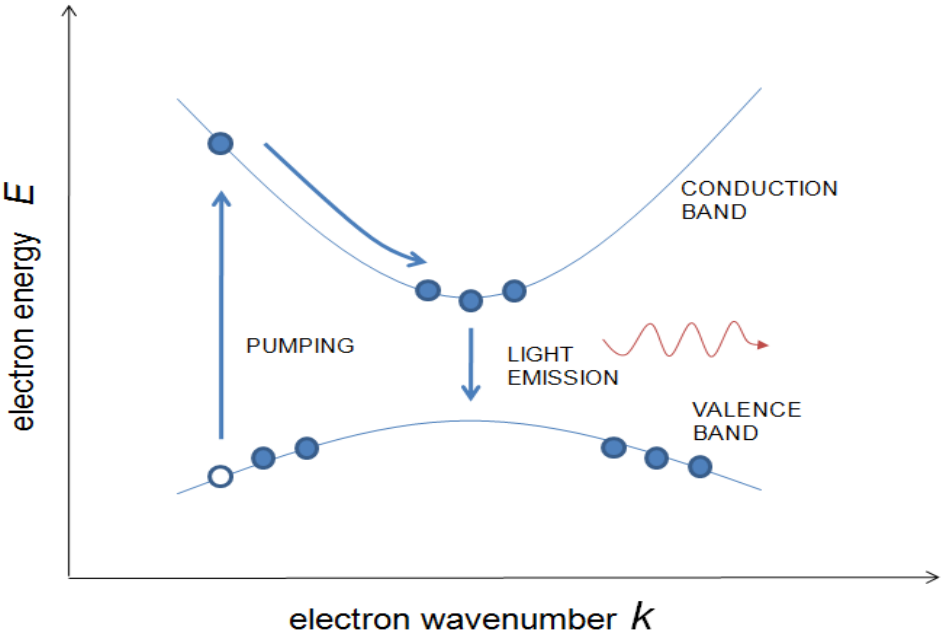

Figure 2.3 Energy bands in semiconductors

The population inversion in a semiconductor laser diode is produced when a p-doped and a n-doped semiconductor material are joined together. The n-doped material contains an excess of electrons and the p-doped material has an excess of holes. When a voltage is applied across the junction it produces an electrical current flow across it. The electrons and holes meet within the junction due to the opposite charges, recombine via spontaneous and stimulated recombination, emit radiation, and produce a population inversion generating photons.

The energy gap typically corresponds to a wavelength near the infrared region (Figure 2.3), therefore most semiconductors radiate in near infrared region and are not transparent in the visible spectral region [26]. The semiconductor material acts both as a gain medium and an optical resonator. Photons leaving the cavity through light emission form the output of a laser.

A key characteristic of a semiconductor laser is the light current curve. It represents the output optical power versus the pump current (Figure 2.4). The larger is its slope, or the closer is the starting point of the curve to the origin, the better is the laser diode as the output optical power is higher for smaller currents injected on the laser.

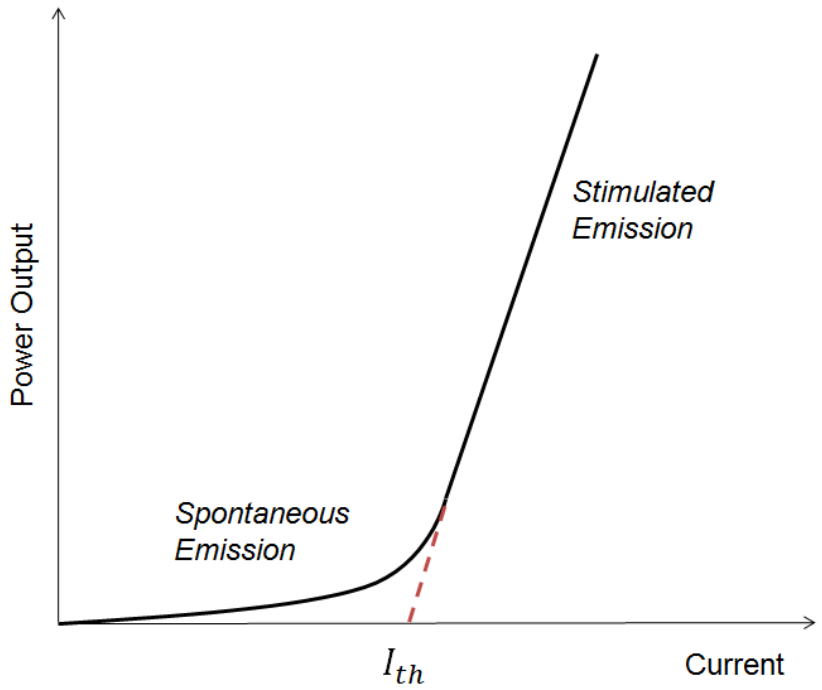

Figure 2.4 Representation of the output power versus injection current in a semiconductor diode laser

Threshold current is one of the most important basic parameters of laser diodes. It specifies the degree at which they emit light when current is injected into the devices. It represents the moment that, as the injected current is increased, the laser first demonstrates stimulated emission. The spontaneous emission increases very gradually until it begins to emit stimulated radiation, which is the onset of laser action. Threshold current is the exact current value at which this phenomenon takes place. It is generally desirable that the threshold current be as low as possible, resulting in a more efficient device. Thus, a threshold current is one measure used to quantify the performance of a laser diode.

Threshold current is dependent on the semiconductor material from which the device is fabricated and the general design of the structure of the device waveguide. However, it is also dependent on the size and area of a laser device. One laser diode could demonstrate a much higher threshold current than another device and still be considered a much better laser due to the area of the device. A laser that is wider or longer requires more electrical power to reach the onset of laser action than a laser of a smaller area. As a result, when comparing the threshold current values of different devices, it is more appropriate to talk about threshold current density rather than threshold current and it is necessary to accurately measure the area of the laser through which current is being injected. Threshold current density J_{th} is determined by dividing the experimentally obtained threshold current value I_{th} by the cross-sectional area of the laser gain medium. However, when comparing the laser optical output power for different

temperatures, I_{th} is an accurate measurement to quantify the performance of that individual laser.

One of the major drawbacks in the use of laser diodes is its strong dependence of the temperature. In most applications, diode lasers are required to be placed in small equipment and sensors. Due to their small packaging, the heat generated under operation builds up easily and therefore in most of its applications there is the need to be cool down to the laser efficient working temperature. Furthermore, it is normally required to quickly dissipate the generated heat as inefficient heat dissipation can cause thermal stresses in the laser diode, and eventually cause irreversible damage to the laser.

Early laser diodes experienced extremely short lifetimes however crystal growth techniques and power systems have improved their life expectancy. Unfortunately, system reliability will always be affected by two major forms of degradation, gradual and catastrophic. Increasing the junction temperature by 10ºC approximately halves the expected mean-time to failure of the laser [14]. Although gradual degradation is laser diodes cannot be eliminated, several techniques can be used to extend a structure's lifetime, among which an effective heat sinking of the substrate to lower the temperature of the active region.

Inefficient cooling packaging design can result in a poor product quality as the temperature of the device core has a direct influence on the output wavelength and band gap of laser light. It is proven in practical situations that for every 3ºC of change of temperature in the laser diode core, the wavelength of the laser light can change nearly 1 nm [27].

As the temperature of a laser diode increases, the refractive index of the semiconductor material itself changes. Since the resonant wavelength of a cavity depends on the refractive index of the material, the wavelength shifts toward the red as temperature of the device increases. The output spectrum of a semiconductor laser is a function of output power, temperature and modulation conditions. From the point of view of optical systems design it is important to know the peak wavelength λ_p and spectral width $\Delta\lambda$ over the range of likely operating conditions. The laser operates at one or more of its longitudinal mode wavelengths. The longitudinal modes correspond to the wavelengths at which there are an integral number of half-wavelengths along the length of the laser cavity. The spacing between the modes $\delta\lambda$ is therefore given by:

$$\delta\lambda = \frac{\lambda^2}{2Ln} \tag{2.4}$$

where L is the length of the laser and n the effective refractive index.

The wavelength of the light responds to temperature changes because the optical path length of the cavity, the refractive index and the gain curve are temperature dependent. As temperature increases the peak of the laser gain spectrum moves towards longer wavelengths (because of

the reducing band gap of the semiconductor). The effective refractive index n also slowly increases. The overall width of the spectrum $\Delta\lambda$ depends on the quality factor (finesse) of the laser cavity [28].

The performance of laser diode is highly dependent on operating conditions. High power diode lasers convert electric energy into light energy at about 10% - 50% efficiency. The remaining amount of energy is emitted as waste heat and must be quickly dissipated. In addition, the output power of the laser light decreases as temperature in the laser diode core increases.

The increase in junction temperature forces an increase in the threshold current necessary to maintain the diode in the lasing region of the power-current spectrum. In general terms the threshold current tends to increase with temperature, the temperature dependence of the threshold current density J_{th} being approximately exponential [29] for most common structures. It is given by:

$$J_{th} = I_z \exp\frac{T}{T_0} \tag{2.5}$$

where T is the device absolute temperature and T_0 is the threshold temperature coefficient which is a characteristic temperature describing the quality of the material, but which is also affected by the structure of the device.

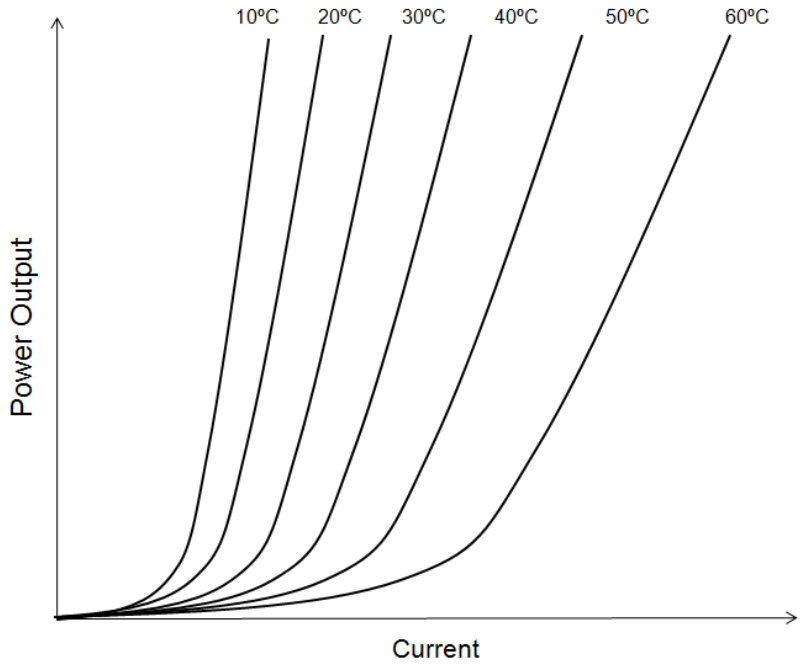

Figure 2.5 Illustrative variation of the output power of a semiconductor laser with temperature based on [28]

At a constant current, the radiated power would be significantly reduced as the temperature rises. The changing of the output curve with the temperature could even lead the device to leave the lasing region and slip back to LED radiation or drive the diode into a non-linear region.

It is critical to maintain constant optical output for laser diodes addressing high speed, fiber optic transmitter applications. Establishing a proper laser bias current is necessary to minimize laser turn-on/off delay and relaxation oscillation. Appropriate laser biasing also limits the sensitivity penalty of optical receivers introduced by inadequate extinction ratio, r_e:

$$r_e = \frac{P_1}{P_0} \tag{2.6}$$

where:

P_1 – "1" power level

P_0 – "0" power level

The extinction ratio is used to describe optimal biasing conditions and how efficiently available laser transmitter power is converted to modulation power. When used to describe the performance of a device like the laser diode, is simply the ratio of the energy (power) used to transmit a logic level "1", to the energy used to transmit a logic level "0" [30].

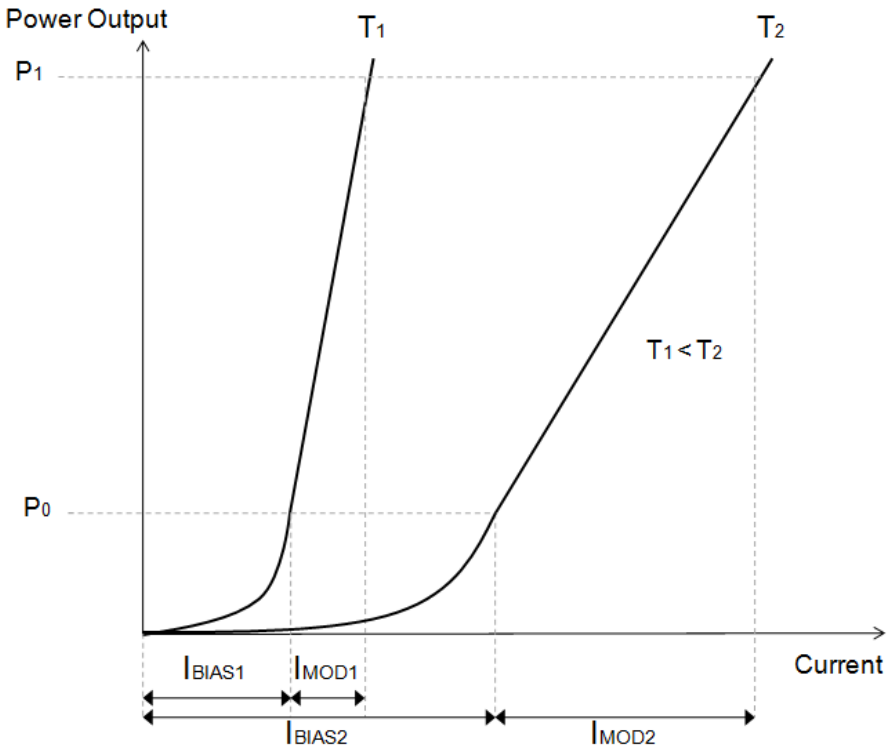

Figure 2.6 Laser behaviour changes with temperature increase

A well-controlled laser modulation current (corresponding to the logic level "1", P_1) ensures that the optical-power budget is met without exceeding the overload level. Figure 2.6 shows the driving current and optical output behavior of a typical laser diode. The laser threshold increases and the slope efficiency decreases as the operating temperature goes up, consequently, it's needed an increased amount of bias current and modulation current to maintain a constant laser emission [30].

Therefore it is necessary to pay substantial attention to thermal dissipation in order to provide efficient heat-sinking arrangements to achieve low operating currents. Lowering J_{th} and improving its temperature stability have been important objectives in the development of semiconductor lasers. Adequate heat sinking along with consideration of the working environment is essential so that devices operate reliably over the anticipated current range [31].

2.2. THERMAL MANAGEMENT TECHNIQUES

The components of a laser system produce a substantial amount of thermal energy which must be dissipated in order to keep the components within their safe operation temperature limits and avoid performance loss and damage. Therefore, cooling methods must be used to dissipate the heat from the core of laser diode and different cooling methods can be adopted in the laser diode packaging. Laser cooling techniques can be classified into different categories from passive to active cooling processes. Efficient cooling methods can dissipate the heat generated to maintain the laser action and its temperature. Laser diode cooling is a crucial concern for designing diode lasers and also to dissipate the high heat flux generated from it.

Passive cooling relies for the most part on heat conduction and natural convection and is usually done by the use of heat sinks. Passive heat sinks can be used to decrease the temperature of the laser by attaching the heat sink, usually made of copper or aluminum, to the laser package. This attachment is made using thermal adhesive materials to securely place the heat sink to the heat source. As the thermal conductivity of a metal is much higher than the thermal conductivity of the air, it increases the ability to radiate heat. Passive heat sinks alone are usually found in low-power lasers that do not reach very high temperatures when functioning therefore not requiring a sensitive control of its temperature. The total rate of heat dissipation, the dimensions, the attachment method, type of the convection, and the direction of the airflow are the major factors affecting the selection of the heat sink. Even though passive cooling has some irrefutable advantages including low complexity, low cost and high reliability, it also has disadvantages when compared to other active cooling solutions, as low heat removal, bulkiness, and the inability to cool below ambient temperature.

Active cooling is typically more expensive than passive cooling and involves moving parts or the input of electrical power. This method actively pumps heat from a heat source to a heat sink. Some common forms of active cooling involve fan cooled heat sinks and thermoelectric coolers. Thermoelectric coolers are a form of active cooling that offers a unique and promising solution to precisely control the temperature. The thermoelectric cooling uses the peltier effect and is being used due to its advantages, such as precise temperature control, high reliability, small size, low cost, light weight and their capability to selectively target and cool lasers controlling their temperature even below ambient temperature.

Three physical phenomena, the Seebeck, Peltier, and Thomson effects are the foundation behind the operation of a thermoelectric device. Of these the Peltier effect is recognized as the dominant force that permits thermoelectric coolers to function.

At the subatomic level, the Seebeck effect is a consequence of the thermal diffusion of electrons and holes. The thermal diffusion in a material with free electrons is greatest at the hot end. Therefore a buildup of electrons occurs at the cold end creating a charge density.

The relationship created by the Seebeck effect between the voltage potential and the different temperatures at the junctions is given by the Seebeck coefficient, which is an inherent property of the circuit of two dissimilar metals. The relationship between voltage and temperature difference is

$$V = \alpha \Delta T \tag{2.7}$$

where V is the voltage across the junctions of the circuit, α is the Seebeck coefficient and ΔT is the temperature difference across the junctions of the circuit.

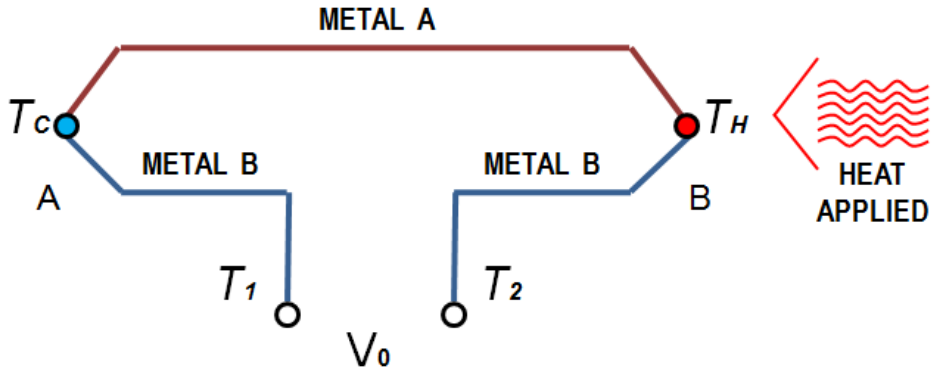

Figure 2.7 Seebeck effect in a thermocouple circuit

In Figure 2.7 the temperature difference across the circuit is expressed as $\Delta T = T_h - T_c$, where T_h and T_c are the hot and cold junctions. With heat applied to thermocouple B, a voltage will appear across to terminals T_1 and T_2.

The Peltier effect is a result of the different energy levels of materials, particularly *n*-type and *p*-type materials. As electrons move from *p*-type material to *n*-type material, electrons jump to a higher energy state absorbing energy, in this case heat, from the surrounding area. The reverse is also true. As electrons move from n type material to p type material, electrons fall to a lower energy state releasing energy to the surrounding area.

The proportionality of the rate of heat transfer Q to amount of current I in the circuit is governed by the Peltier coefficient π as represented in the following equation:

$$Q_{peltier} = \pi I \tag{2.8}$$

Figure 2.8 illustrates the Peltier effect where the direction of heat transfer into the circuit indicates heat absorbed and direction of heat transfer out of the circuit indicates heat emitted. This also states the sign convention of the Peltier coefficient making it positive for heat entering the circuit and negative for heat leaving the circuit. If difference in potential is applied to terminals T_1 and T_2 an electrical current I will flow in the circuit. As a result of the current flow, a cooling effect will occur at thermocouple junction A where heat is absorbed and a heating effect will occur at junction B where heat is expelled. The Peltier effect is reversible between heat and electricity, meaning that the effects either of producing heat transfer from electricity or producing electricity from heat transfer are interchangeable without a loss of energy.

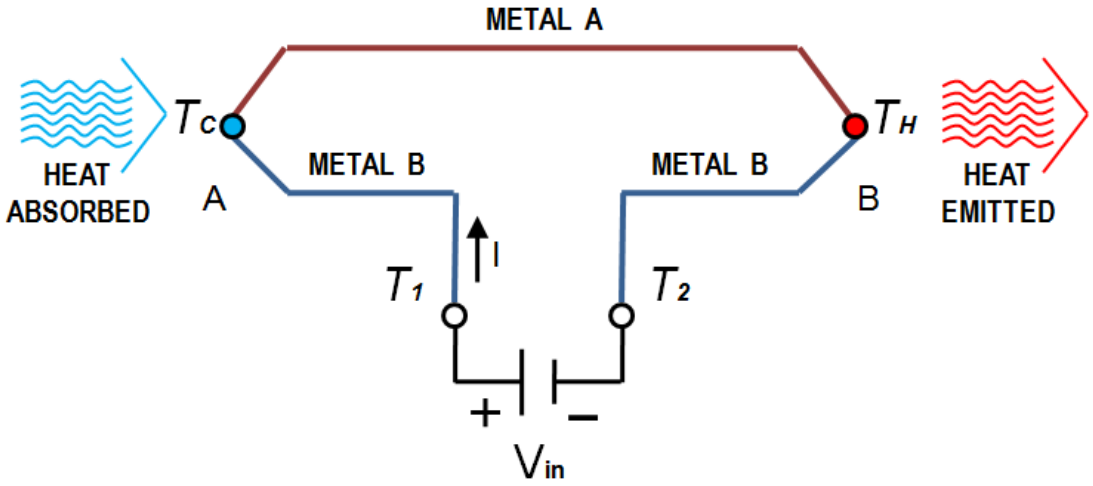

Figure 2.8 Peltier effect in a thermocouple circuit

The Thomson effect is either the absorption or release of a heat from a conductor with a temperature gradient as current is passed through the conductor. This effect is governed by the proportionality of Thomson heat $Q_{Thomson}$ to both current I and temperature difference $\Delta T = T_h - T_c$ using the Thomson coefficient τ as represented in the following equation:

$$Q_{Thomson} = \tau I \Delta T \tag{2.9}$$

Parallel to the Peltier effect the sign convention for the Thomson coefficient is positive for heat absorbed, entering the circuit (metal A) and negative for heat emitted, leaving the circuit (metal B).

The junction of these three effects represents the thermoelectric phenomenon as a whole. These effects are not exclusive to thermoelectric materials alone but are present in all metals and semi-metals however their effects are most observable and practical only in select combinations of dissimilar semi-metals (thermoelectric materials).

2.3. THERMAL DESIGN

All electronic devices produce heat as a side-effect of normal operation. When electrical current flows through a semiconductor or a passive device, a portion of the power is dissipated as heat energy. Besides the damage that excess heat can cause, it also increases the movement of free electrons in a semiconductor, which can cause an increase in signal noise. If the heat is not allowed to dissipate, the device junction temperature will exceed the maximum safe operating temperature specified by the manufacturer. When a device exceeds the specified temperature, semiconductor performance, life, and reliability are reduced. Thermal system designing deals with modeling, simulation, and optimization, and proper selection of the components [32].

Energy is the capacity to perform work. Energy can exist as a numerous forms such as kinetic, potential, electric, chemical, and nuclear. Any form of energy can be transformed into another form, but the total energy always remains the same. This principle, the conservation of energy, was first postulated in the early nineteenth century. It applies to any isolated system. Heat (or heat transferred) is thermal energy that is transferred between two systems due to a temperature difference. Work is the energy transfer associated with a force acting through a distance. Work can exist as a numerous forms such as piston work, shaft work, and electrical work. The rate of work is called power.

The first law of thermodynamics, also known as the conservation of energy, provides a sound basis for studying the relationship among the various forms of energy, total energy, heat, and work. This states that energy cannot be created or destroyed during a process, it can only change forms. The sign convention is illustrated in Figure 2.9.

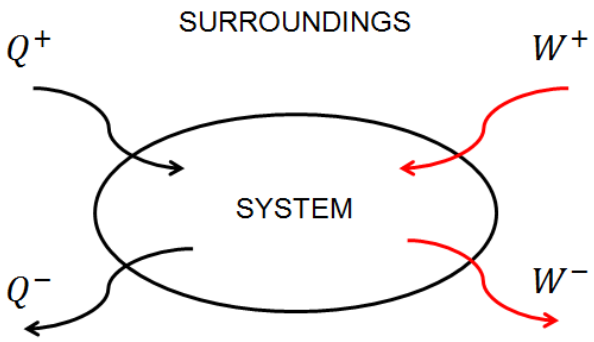

Figure 2.9 Sign convection for work and heat transferred to and from a system

- $Q > 0$ Heat transferred to system
- $Q < 0$ Heat transferred from system
- $W > 0$ Work done on system
- $W < 0$ Work done by system

The first law of thermodynamics for a closed system is given by [32]

$$\Delta U = Q + W \tag{2.10}$$

where ΔU is the internal energy in the system, Q the heat transferred and W the work done on the system.

The change of internal energy U can be expressed thermodynamically:

$$\Delta U = \begin{cases} mc_p \Delta T \; for \; liquids \; and \; solids \\ mc_v \Delta T \; for \; gases \; and \; air \end{cases} \tag{2.11}$$

where m is the mass and c_p and c_v are the specific heat at constant pressure and at constant volume, respectively. ΔT is the temperature variation during the process.

The second law of thermodynamics is associated with the irreversibility, the quality, or the entropy of the process. The classical statements fundamentals are the following:

- Heat is naturally transferred always from a high temperature body to a low temperature body, not vice versa.
- Work is required in order to make heat transfer from a cold temperature body to a high temperature body.
- No heat system has 100 percent thermal efficiency.

- It is impossible to construct a heat system without a heat loss to the environment.

Heat transfer can occur by three modes or mechanisms: conduction, convection, and radiation. Thermal energy involves motions such as the rotation, translation, and vibration of molecules. Temperature measures the average kinetic energy of molecules. Molecules in a warmer object have greater kinetic energy than molecules in a cooler object. When a hot object comes in contact with a cold one, the molecules in the hot object transfer some of their kinetic energy during collisions with molecules of the cold object.

Convection is a combination of the bulk transportation and mixing of macroscopic parts of hot and cold fluid elements, heat conduction within the coolant media, and energy storage. Convection can be due to the expansion of the coolant media in contact with the device. This is called free convection, or natural convection. Convection can also be due to other forces, such as a fan or pump forcing the coolant media into motion. The basic relationship of convection from a hot object to a fluid coolant presumes a linear dependence on the temperature rise along the surface of the solid, known as Newtonian cooling. Therefore:

$$q_c = h_c A_s (T_s - T_m) \tag{2.12}$$

Where q_c is the convective heat flow rate from the surface in W, h_c the coefficient of convective heat transfer in W/(m²K), A_s the surface area for heat transfer in m², T_s the surface temperature in °C and T_m the coolant media temperature in K.

Radiation is the only mode of heat transfer that can occur through a vacuum and is dependent on the temperature of the radiating surface. Although researchers do not yet understand all of the physical mechanisms of radiation heat transfer, it appears to be the result of electromagnetic waves and photonic motion.

The quantity of heat transferred by radiation between two bodies having temperatures of T_1 and T_2 is found by:

$$q_r = \epsilon \sigma F_{1,2} A (T_1^4 - T_2^4) \tag{2.13}$$

Where q_r is the amount of heat transferred by radiation in W, ϵ the emissivity of the radiating surface, σ the Stefan-Boltzmann constant in W/m² K^4, $F_{1,2}$ the shape factor between surface area of body 1 and body 2, A the surface area of radiation in m², T_1 the surface temperature of body 1 in K and T_2 the Surface temperature of body 2 in K.

Unless the temperature of the device is extremely high, or the difference in temperatures is extreme (such as between the sun and a spacecraft), radiation is usually disregarded as a significant source of heat transfer.

Conduction is the transfer of heat from an area of high energy (temperature) to an area of lower relative energy. Conduction occurs by the energy of motion between adjacent molecules and, to varying degrees, by the movement of free electrons and the vibration of the atomic lattice structure. The energy level, or temperature, of a material is related to the vibration level of the molecules within the substance. If the regions are at the same temperature, no heat transfer occurs. In the conductive mode of heat transfer we have no appreciable displacement of the molecules. Fourier's law can be used to predict the rate of heat transfer. The law suggests that the rate of heat transfer be proportional to the area of transfer times the temperature gradient.

In many applications, we use conduction to draw heat away from a device so that convection can cool the conductive surface, such as in an air-cooled heat sink. For a one-dimensional system, the following relation governs conductive heat transfer:

$$q = -\frac{kA_c\Delta T}{L} \tag{2.14}$$

Where q is the heat flow rate in W, k the thermal conductivity of the material in W/m K, A_c the cross-sectional area for heat transfer in m², ΔT the temperature differential and L the length of heat transfer in m.

Fourier's law presents heat transfer as a proportionality equation that depends on the thermal conductivity of the heat transfer media. Thermal conductivity is a physical property that suggests how much heat will flow per unit of time across a unit area. The property of thermal conductivity is important in conduction and convection applications. In some natural convection applications, where we have a confined airspace, heat transfer is actually by conduction, not convection.

2.4. THERMOELECTRIC SYSTEMS

The small dimensions of the laser diode module makes typical methods of cooling impractical or ineffective. Fortunately, the use of thermoelectric cooler (TEC) modules can readily satisfy the need for temperature stability within the small confines of a laser diode package.

TEC modules operate with the Peltier effect, so that by passing an electric current through a junction of dissimilar materials, heat can be created or absorbed at the junction, depending on the direction of the current flow. The operation is similar to the carrier movement in the active region of a laser diode, however, in the case of a TEC, the heavily-doped n-type (negative) and p-type (positive) materials are separated by an electrical conductor.

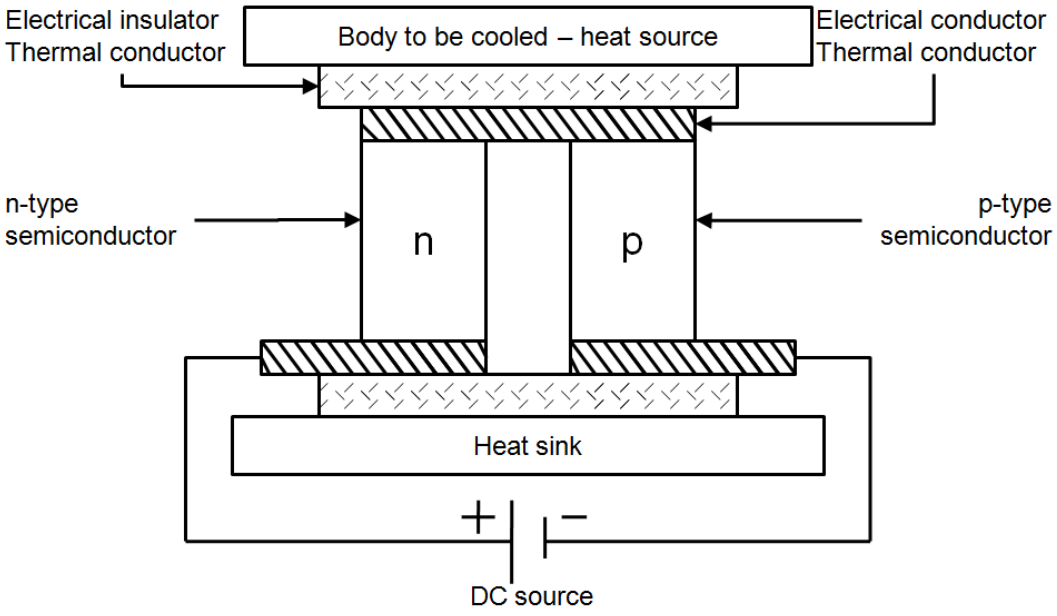

Figure 2.10 Thermoelectric Cooling Couple

To create and sustain the cooling effect, the module is reversed biased, as shown in Figure 2.10. Electrons are pumped from the p-type to n-type region where they are moved from the valence band to the conduction band. Via the classical laws of thermodynamics, work has been done on the electron and therefore heat is absorbed and the junction is cooled. As the junction temperature decreases, heat is drawn from the heat source through an electrical insulator that is a good thermal conductor. The same process holds true for the flow of holes in the opposite direction. Therefore, both carriers work together to remove heat from the junction at a rate proportional to the current applied. In an equal but opposite manner, heat can be produced at the junction by forward biasing the module.

By connecting the doped regions in series electrically and in parallel thermally, the module can heat or cool a system and maintain a stable environment. The basic building block of a thermoelectric couple is one p-type and one n-type thermoelectric element. These thermoelectric couples subsequently become the basis in forming a thermoelectric module.

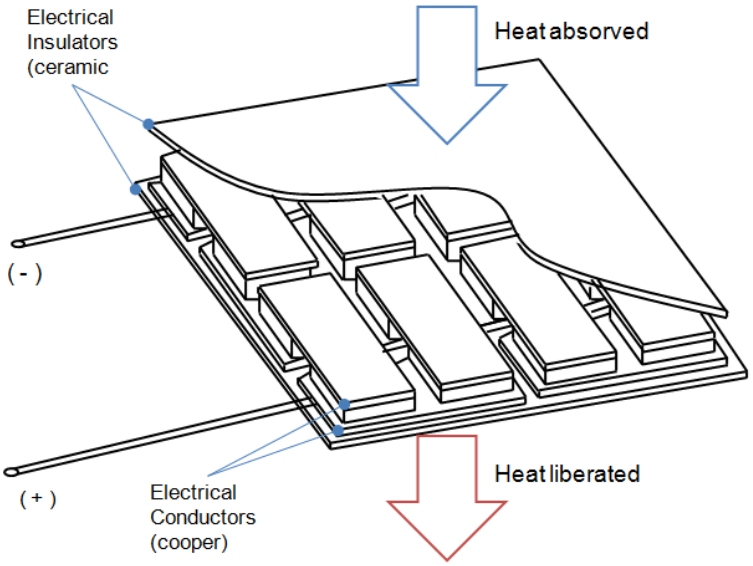

Figure 2.11 Cutaway of a TEC module

Figure 2.11 illustrates a cutaway of a typical thermoelectric module which consists of several thermoelectric couples connected to each other by electrical conductors and kept between two ceramic plates. The electrical conductors are arranged so that the thermoelectric couples are electrically in series with each other.

The ceramic plates act as an electrical insulator and thermal conductor allowing the couples to be thermally in parallel – the top of every couple is subjected to the same constant temperature while the bottom of every couple is at another constant temperature in the case of a TEC as represented in Figure 2.12.

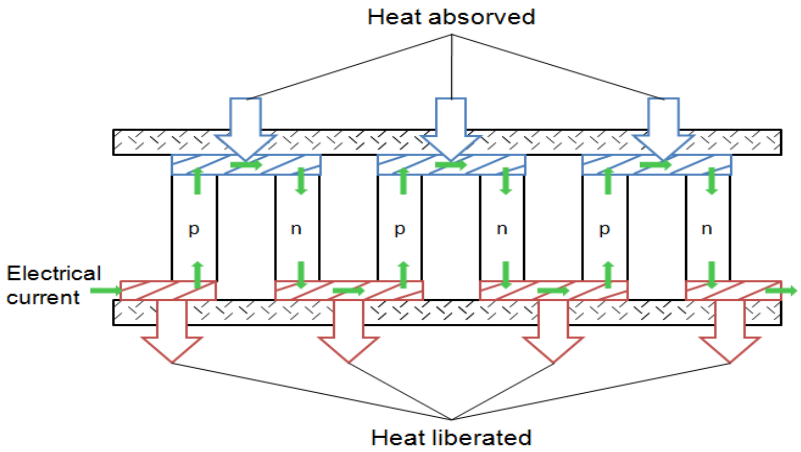

Figure 2.12 Electrical and thermal connectivity of TEC couples within a module

To find the thermoelectric cooler ideal equations let's consider the following equations in vector form to represent general three-dimensional cases. Considering a non-uniformly heated thermoelectric material that has isotropic material properties, the continuity equation for a constant current flux $\vec{J}$ is given as

$$\vec{\nabla} \cdot \vec{J} = 0 \tag{2.15}$$

where $\vec{\nabla}$ is the differential operator with respect to length. The electric field has contributions from both Ohm's Law and the Seebeck effect, which is obtained by differentiating equation (2.7) with respect to length. The electric field is given as

$$\vec{E} = \vec{J}\rho + \alpha\vec{\nabla}T \tag{2.16}$$

The heat flow density vector $\vec{q}$ is expressed as

$$\vec{q} = \alpha T\vec{J} - k\vec{\nabla}T \tag{2.17}$$

where T is the temperature of the heat flux boundary. The $\alpha T\vec{J}$ term is the Peltier heat contribution while the $k\vec{\nabla}T$ term gives heat transfer from Fourier's Law of conduction. The general heat diffusion equation as a function of time is given by

$$-\vec{\nabla} \cdot \vec{q} + \dot{q} = \rho_m c_p \frac{\partial T}{\partial t} \tag{2.18}$$

where $\dot{q}$ is the heat generated per unit volume, ρ_m is the mass density of the material, c_p is the specific heat capacity and $\frac{\partial T}{\partial t}$ is the rate of change of temperature with respect to time. Only considering steady state conditions causes the time dependent term $\frac{\partial T}{\partial t}$ to become zero. Equation (2.18), after rearranging, reduces to

$$\dot{q} = \vec{\nabla} \cdot \vec{q} \tag{2.19}$$

The relationship between the rate of thermal energy generated and electrical power is expressed as

$$\dot{q} = \vec{E} \cdot \vec{J} = J^2\rho + \vec{J} \cdot \alpha\vec{\nabla}T \tag{2.20}$$

Equations (2.17) and (2.20) can be substituted into equation (2.19) to obtain

$$\vec{\nabla} \cdot (k\vec{\nabla}T) + J^2\rho - T\frac{d\alpha}{dT}\vec{J} \cdot \vec{\nabla}T = 0 \tag{2.21}$$

where $J^2\rho$ is a form of Joule heating that occurs in all current carrying materials due to the interaction between electrical current and resistance. The term $T\frac{d\alpha}{dT}$ refers to the Thomson coefficient. Previous studies indicate that exact solutions that include the integral of the Thomson coefficient as a function of temperature show almost exact agreements with exact solutions that neglect the Thomson coefficient [33]. Therefore we will assume that the Thomson coefficient is negligible and that the Seebeck coefficient is independent of temperature.

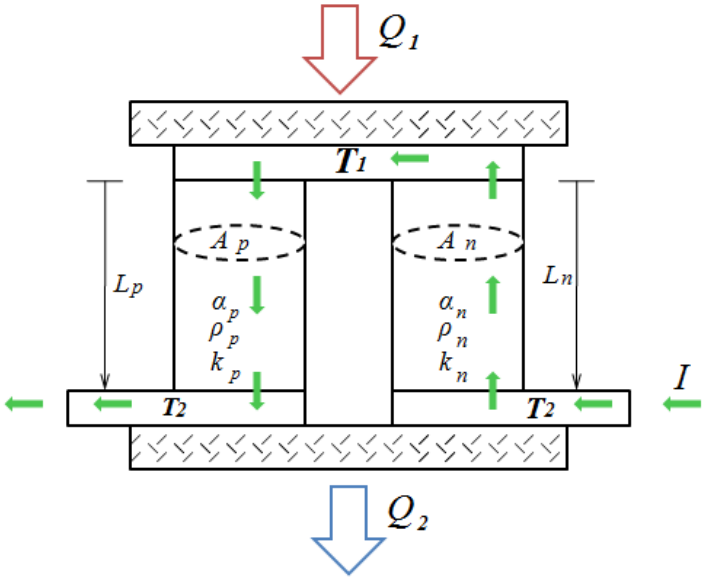

Figure 2.13 Thermoelectric cooling couple properties

The constituent material properties of a thermoelectric couple, Seebeck coefficient α, electrical resistivity ρ and thermal conductivity K, and the geometric information, longitudinal length L and lateral cross-sectional area A, are represented in Figure 2.13. Both elements n-type and p-type experience the same junction temperatures T_1 and T_2 at opposite ends where uniform heat fluxes occur and both elements are subjected to the same magnitude of current I. The heat transfer rates Q_1 and Q_2 occur at junctions with temperatures T_1 and T_2, respectively.

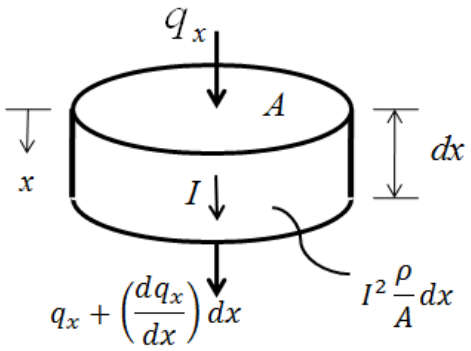

Figure 2.14 Differential Element of a Thermoelectric Element

Consider a differential element of one of the thermoelectric legs with cross sectional area and differential length as shown in Figure 2.14. A uniform current that passes through the differential element with electrical resistivity will evoke Joule heating effects. It is now assumed that Joule heating is the only source of internal energy generated within the differential element.

Adopting the sign convention that heat flow into element is positive, considering only one-dimension and rearranging equation (2.19), the heat balance on the differential element now becomes

$$q_x - \left(q_x + \left(\frac{dq_x}{dx}\right)\right)dx + I^2\frac{\rho}{A}dx = 0 \tag{2.22}$$

where q_x is the heat flow. Equation (2.17), multiplied by the area normal to the direction of heat flux A, becomes

$$q_x = \alpha T(x)I - kA\frac{dT}{dx} \tag{2.23}$$

where $I = J_x A$ and the temperature T is a function of position x. Differentiating equation equation (2.23) with respect to x becomes

$$\frac{dq_x}{dx} = -kA\frac{d}{dx}\left(\frac{dT}{dx}\right) \tag{2.24}$$

Substituting equation (2.24) into equation (2.22) and rearranging gives

$$kA\frac{d}{dx}\left(\frac{dT}{dx}\right) = -I^2\frac{\rho}{A} \tag{2.25}$$

Integrating equation (2.25) gives

$$kA \int d\left(\frac{dT}{dx}\right) = -I^2 \frac{\rho}{A} \int dx \;\rightarrow\; \frac{dT}{dx} = -I^2 \frac{\rho}{kA^2} x + C_1 \tag{2.26}$$

Integrating equation (2.26) again from $x = 0$ to $x = L$ with the boundary conditions $T(x = 0) = T_1$ and $T(x = L) = T_2$ leads to

$$\int_{T_1}^{T_2} dT \; = -I^2 \frac{\rho}{kA^2} \int_0^L x + \int_0^L x\, C_1 \rightarrow T_2 - T_1 = -I^2 \frac{\rho}{2kA^2} L^2 + C_1 L \tag{2.27}$$

Equation (2.27) can be rearranged to obtain the constant of integration C_1 as

$$C_1 = \frac{T_2 - T_1}{L} + I^2 \frac{\rho}{2kA^2} L \tag{2.28}$$

Substituting equation (2.28) into (2.26) at $x = 0$ becomes

$$\left.\frac{dT}{dx}\right|_{x=0} = \frac{T_2 - T_1}{L} + I^2 \frac{\rho}{2kA^2} L \tag{2.29}$$

Now substituting equation (2.28) into (2.26) at $x = L$ leads to

$$\left.\frac{dT}{dx}\right|_{x=L} = \frac{T_2 - T_1}{L} - I^2 \frac{\rho}{2kA^2} L \tag{2.30}$$

Substituting equation (2.29) into (2.23) yields

$$q_{x=0} = \alpha T_1 I - \frac{1}{2} I^2 \frac{\rho L}{A} + \frac{kA}{L}(T_1 - T_2) \tag{2.31}$$

For their respective elements, p-type and n-type, equation (2.31) becomes

$$q_{p,x=0} = \alpha_p \, T_1 I - \frac{1}{2} I^2 \frac{\rho_p L_p}{A_p} + \frac{k_p A_p}{L_p}(T_1 - T_2) \tag{2.32}$$

$$q_{n,x=0} = -\alpha_n T_1 I - \frac{1}{2} I^2 \frac{\rho_n L_n}{A_n} + \frac{k_n A_n}{L_n}(T_1 - T_2) \tag{2.33}$$

The Seebeck coefficient for the n-type element is negative because it is negatively doped and carries a preceding negative sign in order to validate the thermoelectric equations. Similarly, the heat transfer equations at $x = L$ for the p-type and n-type, with $T(x = L) = T_2$ and equation (2.30), are

$$q_{p,x=L} = \alpha_p \, T_2 I + \frac{1}{2} I^2 \frac{\rho_p L_p}{A_p} + \frac{k_p A_p}{L_p}(T_1 - T_2) \tag{2.34}$$

$$q_{n,x=L} = -\alpha_n T_2 I + \frac{1}{2} I^2 \frac{\rho_n L_n}{A_n} + \frac{k_n A_n}{L_n} (T_1 - T_2) \tag{2.35}$$

From Figure 2.14, realizing that $Q_1 = q_{p,x=0} + q_{n,x=0}$ and $Q_2 = q_{p,x=L} + q_{n,x=L}$, the respective heat transfer rates at junctions of the thermoelectric couple are

$$Q_1 = \left(\alpha_p - \alpha_n\right) T_1 I - \frac{1}{2} I^2 \left(\frac{\rho_p L_p}{A_p} + \frac{\rho_n L_n}{A_n} \right) + \left(\frac{k_p A_p}{L_p} + \frac{k_n A_n}{L_n} \right) (T_1 - T_2) \tag{2.36}$$

$$Q_2 = \left(\alpha_p - \alpha_n\right) T_2 I - \frac{1}{2} I^2 \left(\frac{\rho_p L_p}{A_p} + \frac{\rho_n L_n}{A_n} \right) + \left(\frac{k_p A_p}{L_p} + \frac{k_n A_n}{L_n} \right) (T_1 - T_2) \tag{2.37}$$

The material properties of the p-type and n-type elements can be related together with the Seebeck coefficient α, total electrical resistance R and thermal conductance K using the following equations:

$$\alpha = \alpha_p - \alpha_n \tag{2.38}$$

$$R = \frac{\rho_p L_p}{A_p} + \frac{\rho_n L_n}{A_n} \tag{2.39}$$

$$K = \frac{k_p A_p}{L_p} - \frac{k_n A_n}{L_n} \tag{2.40}$$

Using equations (2.38), (2.39) and (2.40), equations (2.36) and (2.37) can be simplified so that we are able to reach equations (2.41) and (2.42) that are known as the Ideal Equations [34]:

$$Q_1 = \alpha T_1 I - \frac{1}{2} I^2 R + K(T_1 - T_2) \tag{2.41}$$

$$Q_2 = \alpha T_2 I + \frac{1}{2} I^2 R + K(T_1 - T_2) \tag{2.42}$$

The first term in both equations $\alpha T I$ is known as the peltier/seebeck effect and it is reversible. This is the driving force of thermo power, i.e. the stronger this parameter, the greater the effect of cooling. The second term $\frac{1}{2} I^2 R$ is the Joule heating term which comes from the interaction between electrical current and the TEC electric resistance and works against the primary objective to cool or generate power. The last term $K(T_1 - T_2)$ is the thermal conduction term which occurs due to a temperature difference in any material and also works against the cooling power of TECs. Both the Joule heating and conduction terms are irreversible.

The ideal equation is formulated under the assumptions that the electrical and thermal contact resistances, the Thomson effect (temperature-dependent Seebeck coefficient), and the radiation and convection heat transfer are negligible [35],[36].

Most manufacturers insulate the outlying sides of the thermoelectric module to prevent convective losses yet, convection and radiation losses take place in the air breaches of the two ceramic plates, the regions unoccupied by thermoelectric elements. The smaller the fill factor the larger the potential losses through convection and radiation within a module. However the radiation and convection heat transfer is sufficiently small for the moderate temperature differences between the hot and cold junction temperatures and the surrounding temperature in typical commercial cooler modules so that it's acceptable to disregard in the ideal equation.

When the Thomson heat is positive, it plays the role of cooling in the interior to reduce the effect of Joule heat and enhance the cooling capacity of the TEC while a negative Thomson coefficient reduces its performance. When comparing the value of Joule heat and Thomson heat, Joule heat much larger than Thomson heat [37]. For this reason the Joule heat dominates in the internal thermal mechanism. The assumption of the negligible Thomson coefficient has been proven to be appropriate for either the moderate currents or the moderate temperature differences [33].

It is also assumed that the interfaces between the ceramic substrates that sandwich the thermoelectric elements as well as the electrical conductors that connect the couples together are perfect. In reality, due to imperfections during manufacturing and assembly, there are electrical contact resistances between the conductors and the junctions of each thermoelectric element and there are thermal resistances through the ceramic plates and electrical conductors. The major errors between the measurements and the ideal equation lie on the electrical and thermal contact resistances [35].

3. THERMAL MODEL

Using cold and hot junction temperatures, T_C and T_H, instead of temperatures T_1 and T_2, equations (2.41) and (2.42) become:

$$Q_C = \alpha T_C I - \frac{1}{2} I^2 R - K(T_H - T_C) \tag{3.1}$$

$$Q_H = \alpha T_H I + \frac{1}{2} I^2 R - K(T_H - T_C) \tag{3.2}$$

The heat transfer rates Q_C and Q_H can be expressed in terms of the heat capacities $[\mathrm{J\,K^{-1}}]$ C_C and C_H and the rate of change of the temperature $[\mathrm{K\,s^{-1}}]$ dT_C and dT_H in the cold and hot junctions respectively:

$$Q_C = C_C \frac{dT_C}{dt} \tag{3.3}$$

$$Q_H = C_H \frac{dT_H}{dt} \tag{3.4}$$

An object's heat capacity is defined as the ratio of the amount of heat energy transferred to an object and the resulting increase in temperature of the object. It is also related to the mass specific heat capacity c_m $[\mathrm{J\,kg^{-1}\,K^{-1}}]$, an intrinsic characteristic of a particular substance:

$$C = c_m m \tag{3.5}$$

3.1. PELTIER MODULE

Figure 3.1 represents a simplified model for the TEC module that will be used in this study. This model goes according to the same assumptions on which the ideal equations were formulated, that the electrical and thermal contact resistances, the Thomson effect and the radiation and convection heat transfer are negligible. It considers however the heat transfer by conduction with the surrounding ambient temperature.

Based on the ideal equations (3.1) and (3.2) and equations (3.3), (3.4) and (3.5), the TEC module can be defined by the incoming and outgoing flows of thermal power between the cold and hot side and with the environment as represented in equations (3.6) and (3.7). The last terms $K_C(T_0 - T_C)$ and $K_H(T_H - T_0)$ relate to the thermal conduction which occurs due to a temperature difference between the cold and hot junctions with the surrounding ambient.

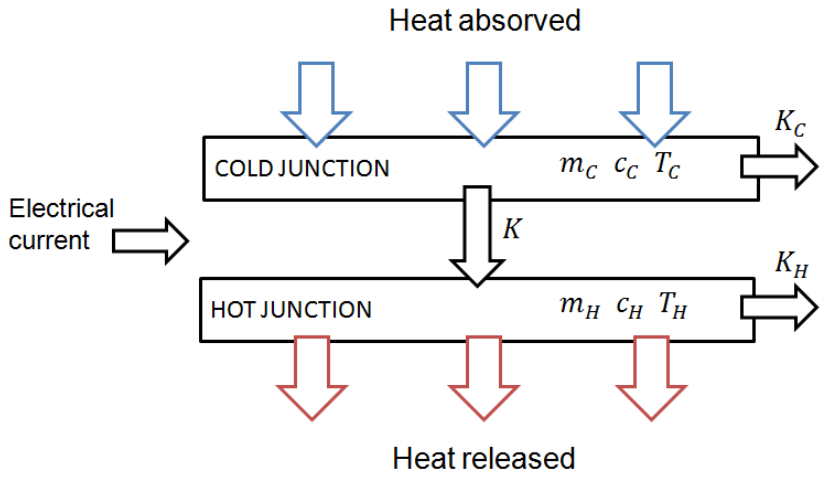

Figure 3.1 Basic thermal model of a TEC module

$$m_C c_C \frac{dT_C}{dt} = -\alpha I_p T_C + \frac{1}{2} R I_p^2 + K(T_H - T_C) + K_C(T_0 - T_C) \quad (3.6)$$

$$m_H c_H \frac{dT_H}{dt} = \alpha I_p T_H + \frac{1}{2} R I_p^2 - K(T_H - T_C) - K_H(T_H - T_0) \quad (3.7)$$

Where α, R and K are the parameters that describe the performance of the thermoelectric cooler, seebeck coefficient in VK^{-1}, electrical resistance in Ω and the thermal conductance between the cold and hot sides in WK^{-1}, respectively, I_p being the peltier current in A, T_C , T_H and T_0 stand for the temperatures in the cold and hot sides and in the environment in K and K_h

and K_C represent the thermal conductance between the hot and cold sides and the environment in WK^{-1}.

To understand the optimized function of each system is fundamental to perfectly determine each of the parameters of the thermal model that describes it. Some of the parameters of the system are easy to control and determine with simple measurements as the temperature in each element. Other parameters can only be determined by testing how the system responds in controlled conditions.

The values of the temperatures in each of the thermoelectric cooler junctions can be measured using a thermistor as a temperature sensor as it produces a temperature dependent voltage as a result of the thermoelectric effect, and this voltage can be interpreted to measure temperature.

Considering again the system represented in Figure 3.1 and writing equations (3.6) and (3.7) considering now the steady state solution for the system we obtain the following equations:

$$-\alpha I_p T_C + \frac{1}{2} R I_p^2 + K(T_H - T_C) + K_C(T_0 - T_C) = 0 \tag{3.8}$$

$$\alpha I_p T_H + \frac{1}{2} R I_p^2 - K(T_H - T_C) - K_H(T_H - T_0) = 0 \tag{3.9}$$

Unifying both equations we can obtain one single equation that represents the steady state of the system:

$$\alpha I_p T_H - \alpha I_p T_C + R I_p^2 - K_C(T_0 - T_C) - K_H(T_H - T_0) = 0 \tag{3.10}$$

Solving the equation in terms of T_H we obtain the equation that describes the temperature in the hot side of the thermoelectric cooler for the steady state:

$$T_H = \frac{-K_c(T_0 - T_c) - K_H T_0 - R {I_p}^2 + \alpha I_p T_c}{\alpha I_p - K_H} \tag{3.11}$$

Replacing T_H in equation (3.8) by the result obtained in equation (3.11) we find the equation that describes the temperature in the cold side of the thermoelectric cooler with respect to the parameters of the TEC, and the environmental conditions:

$$T_c = \frac{\frac{1}{2} R {I_p}^3 \alpha - \frac{1}{2} R I_p^2 K_H - K R {I_p}^2 + K_c T_0 \alpha I_p - K_C T_0 K - K K_H T_0 - K_C T_0 K_H}{-\alpha^2 {I_p}^2 + \alpha I_p K_H - K_C \alpha I_p + K K_C + K K_H + K_C K_H} \tag{3.12}$$

Considering now the case of no current applied to the system, we obtain a nonhomogeneous linear system of differential equations:

$$\frac{dT_C}{dt} = \left(-\frac{K + K_C}{m_C C_C}\right) T_C + \frac{K}{m_C C_C} T_H + \frac{K_C}{m_C C_C} T_0 \tag{3.13}$$

$$\frac{dT_H}{dt} = \frac{K}{m_H C_H} T_C + \left(-\frac{K_H + K}{m_H C_H}\right) T_H + \frac{K_H}{m_H C_H} T_0 \tag{3.14}$$

The system obtained can be written as the equivalent matrix system $x' = A(t)x + f(t)$, where

$$x = \begin{pmatrix} T_C \\ T_H \end{pmatrix}, \qquad A = \begin{pmatrix} -\frac{K + K_C}{m_C C_C} & \frac{K}{m_C C_C} \\ \frac{K}{m_H C_H} & -\frac{K_H + K}{m_H C_H} \end{pmatrix}, \qquad f = \begin{pmatrix} \frac{K_C}{m_C C_C} \\ \frac{K_H}{m_H C_H} \end{pmatrix} T_0$$

that admits solutions $x(t)$ as represented in equation (3.15) where the two first terms correspond to the homogeneous solution and $x_p(t)$ represents a particular solution of the matrix system.

$$x(t) = c_1 e^{\lambda_1 t} u_1(t) + c_2 e^{\lambda_2 t} u_2(t) - x_p(t) \tag{3.15}$$

The solution obtained for the system with no current applied is a second order exponential decay with exponential time constants $t_1(t_2) = -\frac{1}{\lambda_1(\lambda_2)}$.

Considering the elements of the matrix A, $a = \frac{K+K_C}{m_C C_C}$, $b = \frac{K}{m_C C_C}$, $c = \frac{K}{m_H C_H}$ and $d = \frac{K_H+K}{m_H C_H}$, we obtain the expressions for the parameters λ_1 and λ_2 as follows,

$$\lambda_{1,2} = \frac{-(a+d) \pm \sqrt{(a+d)^2 - 4(ad - cb)}}{2} \tag{3.16}$$

Replacing the elements of the matrix A for their corresponding system parameters dependency we finally obtain:

$$\lambda_1 = \frac{-\left(\frac{K + K_C}{m_C C_C} + \frac{K_H + K}{m_H C_H}\right) + \sqrt{\left(\frac{K + K_C}{m_C C_C} + \frac{K_H + K}{m_H C_H}\right)^2 - 4\left(\frac{K + K_C}{m_C C_C}\frac{K_H + K}{m_H C_H} - \frac{K}{m_H C_H}\frac{K}{m_C C_C}\right)}}{2} \tag{3.17}$$

$$\lambda_2 = \frac{-\left(\frac{K + K_C}{m_C C_C} + \frac{K_H + K}{m_H C_H}\right) - \sqrt{\left(\frac{K + K_C}{m_C C_C} + \frac{K_H + K}{m_H C_H}\right)^2 - 4\left(\frac{K + K_C}{m_C C_C}\frac{K_H + K}{m_H C_H} - \frac{K}{m_H C_H}\frac{K}{m_C C_C}\right)}}{2} \tag{3.18}$$

Equations (3.8), (3.9), (3.17) and (3.18) will be afterwards used to determine the values of the unknown parameters that describe the system. These unknown parameters will enable the designer to better understand the system.

3.2. SEMICONDUCTOR LASER AND ITS THERMOELECTRIC COOLER

Introducing now the laser diode and the optional but eventually needed heat sink to the system we obtain a system more complex than the previously considered. This system, represented in Figure 3.2, describes the heat exchanges between all the components, laser, thermoelectric cooler, heat sink and the environment. While this system is more complex than the previously one it is needed to understand the behavior of the temperatures in each element of the system.

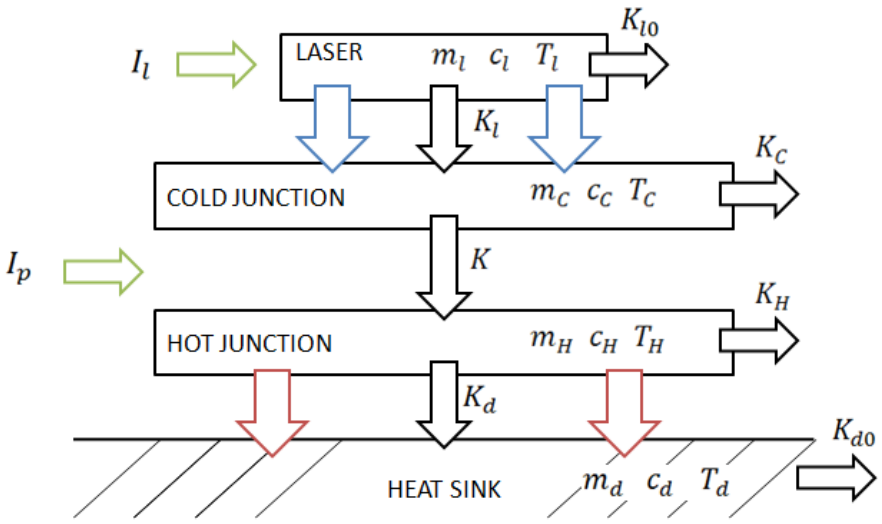

Figure 3.2 Thermal model for the semiconductor laser its TEC module and heat sink

Based on the previous equations (3.6) and (3.7), following the same assumptions as in the thermal model of the thermoelectric cooler alone and also considering the heat transfer by conduction with the surrounding ambient temperature, the system represented on Figure 3.2 can be described by the following series of equations:

$$m_l c_l \frac{dT_l}{dt} = P_l - K_l(T_l - T_C) - K_{l0}(T_l - T_0) \tag{3.19}$$

$$m_C c_C \frac{dT_C}{dt} = -\alpha I_p T_C + \frac{1}{2} R I_p^2 + K(T_H - T_C) + K_C(T_0 - T_C) + K_l(T_l - T_C) \tag{3.20}$$

$$m_H c_H \frac{dT_H}{dt} = \alpha I_p T_H + \frac{1}{2} R I_p^2 - K(T_H - T_C) - K_H(T_H - T_0) - K_d(T_H - T_d) \tag{3.21}$$

$$m_d c_d \frac{dT_d}{dt} = K_d(T_H - T_d) - K_{d0}(T_d - T_0) \tag{3.22}$$

Like in the previous model α, R and K are the parameters that express the performance of the thermoelectric cooler, seebeck coefficient in VK^{-1}, electrical resistance in Ω and the thermal conductance between the cold and hot sides in WK^{-1}. The variable I_p represents the peltier current in Ampere while T_C , T_H and T_0 stand for the temperatures of the cold and hot junctions and the environment in K. The parameters K_h, K_C, K_{l0} and K_{d0} represent the thermal conductance between each of the elements, the hot and cold junctions, the laser and the heat sink with the environment, respectively, in WK^{-1}

Analyzing Figure 3.2 there are five different temperatures that describe the system that involves a diode laser with a thermoelectric cooler, the temperature of the laser, the temperatures of the hot and cold junctions of the thermoelectric cooler, the temperature of the heat sink, T_d, and the environment temperature, T_0. While temperatures are normally an easy parameter to measure, the real configuration of the system and the fact that some of the elements are mounted together in the laser package an accurate individual measurement is not always doable.

To simplify these measurements and consequently the thermal model, the system considered is represented in Figure 3.3.

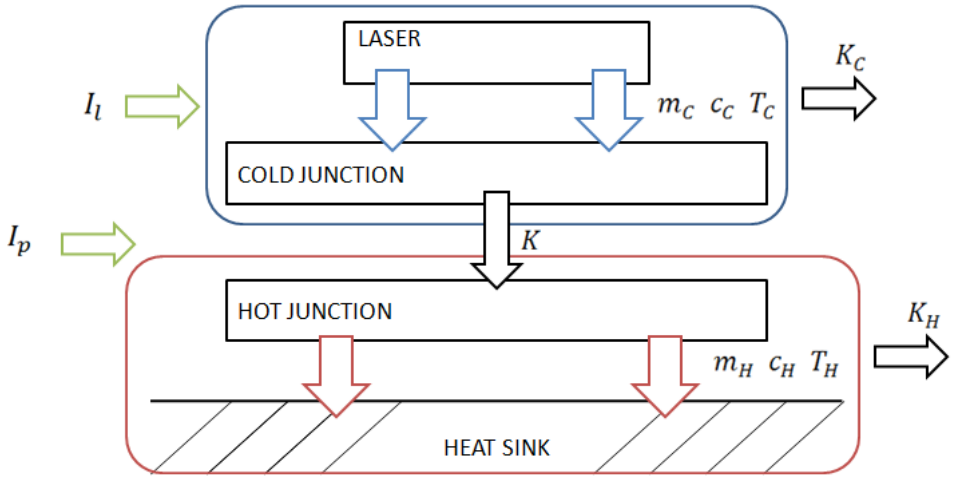

Figure 3.3 Simplified thermal model for a semiconductor laser with a thermoelectric cooler and a heat sink

This simplified model enables a simpler measurement of the temperatures of the system. The hot part of the system will be united into one component as it was in the preceding experiment of the system thermoelectric cooler with a heat sink. As previously this allows us to consider only one temperature for the set hot junction and heat sink and measure it against the junction of the two elements. The temperature T_H, thermal conductivity K_H, mass m_H and heat capacity c_H will refer to the set heat sink and hot junction of the peltier module. Likewise, the cold part of the system will be united into one component so that we can consider only one temperature on the cold side for the set cold junction and laser. The temperature T_C, thermal conductivity K_C, mass m_C and heat capacity c_C will then refer to the set laser and cold junction of the thermoelectric module.

Based on equations (3.6) and (3.7), following the same assumptions as in the thermal model of the thermoelectric cooler alone, considering the heat transfer by conduction with the surrounding ambient temperature and also the laser influence, the system represented on Figure 3.3 can be described by the following series of equations:

$$m_C c_C \frac{dT_C}{dt} = P_l - \alpha I_p T_C + \frac{1}{2} R I_p^2 + K(T_H - T_C) + K_C(T_0 - T_C) \tag{3.23}$$

$$m_H c_H \frac{dT_H}{dt} = \alpha I_p T_H + \frac{1}{2} R I_p^2 - K(T_H - T_C) - K_H(T_H - T_0) \tag{3.24}$$

Where P_l is the optical power of the laser in W, α, R and K are the parameters that describe the performance of the thermoelectric cooler, seebeck coefficient in VK^{-1}, electrical resistance in Ω and the thermal conductance between the cold and hot sides in WK^{-1}, respectively, I_p being the peltier current in A, T_C , T_H and T_0 stand for the temperatures in the cold and hot sides and in the

environment in K and K_h and K_C represent the thermal conductance between the hot and cold sides and the environment in WK^{-1}.

Writing equations (3.23) and (3.24) considering now the steady state solution for the system we obtain the following equations:

$$P_l - \alpha I_p T_C + \frac{1}{2} R I_p^2 + K(T_H - T_C) + K_C(T_0 - T_C) = 0 \tag{3.25}$$

$$\alpha I_p T_H + \frac{1}{2} R I_p^2 - K(T_H - T_C) - K_H(T_H - T_0) = 0 \tag{3.26}$$

Unifying both equations we can obtain one single equation that represents the steady state of the system:

$$P_l + \alpha I_p T_H - \alpha I_p T_C + R I_p^2 - K_C(T_0 - T_C) - K_H(T_H - T_0) = 0 \tag{3.27}$$

Solving the equation in terms of T_H we obtain the equation that describes the temperature in the hot side of the thermoelectric cooler for the steady state:

$$T_H = \frac{-K_c(T_0 - T_c) - K_H T_0 - R {I_p}^2 + \alpha I_p T_c + P_l}{\alpha I_p - K_H} \tag{3.28}$$

Replacing T_H in equation (3.25) by the result obtained in equation (3.28) we find the equation that describes the temperature in the cold side of the thermoelectric cooler with respect to the parameters of the TEC, and the environmental conditions:

$$T_c = \frac{\frac{1}{2} R {I_p}^3 \alpha - \frac{1}{2} R I_p^2 K_H - K R {I_p}^2 + K_c T_0 \alpha I_p - K_C T_0 K - K K_H T_0 - K_C T_0 K_H + K P_l + \alpha I_p P_l - K_H P_l}{-\alpha^2 {I_p}^2 + K_H + K K_C + K K_H + K_C K_H} \tag{3.29}$$

Considering now the case of no current applied to the system, we obtain a nonhomogeneous linear system of differential equations:

$$\frac{dT_C}{dt} = \left(-\frac{K + K_C}{m_C C_C}\right) T_C + \frac{K}{m_C C_C} T_H + \frac{K_C T_0 + P_l}{m_C C_C} \tag{3.30}$$

$$\frac{dT_H}{dt} = \frac{K}{m_H C_H} T_C + \left(-\frac{K_H + K}{m_H C_H}\right) T_H + \frac{K_H}{m_H C_H} T_0 \tag{3.31}$$

The system obtained can be written as the equivalent matrix system $x' = A(t)x + f(t)$, where

$$x = \begin{pmatrix} T_C \\ T_H \end{pmatrix}, \qquad A = \begin{pmatrix} -\frac{K + K_C}{m_C C_C} & \frac{K}{m_C C_C} \\ \frac{K}{m_H C_H} & -\frac{K_H + K}{m_H C_H} \end{pmatrix}, \qquad f = \begin{pmatrix} \frac{K_C T_0 + P_l}{m_C C_C} \\ \frac{K_H}{m_H C_H} T_0 \end{pmatrix}$$

that admits solutions $x(t)$ as represented in equation (3.32) where the two first terms correspond to the homogeneous solution and $x_p(t)$ represents a particular solution of the matrix system.

$$x(t) = c_1 e^{\lambda_1 t} u_1(t) + c_2 e^{\lambda_2 t} u_2(t) - x_p(t) \tag{3.32}$$

The solution obtained for the system with no current applied is a second order exponential decay with exponential time constants $t_1(t_2) = -\frac{1}{\lambda_1(\lambda_2)}$.

Considering the elements of the matrix A, $a = \frac{K+K_C}{m_C C_C}, b = \frac{K}{m_C C_C}, c = \frac{K}{m_H C_H}$ and $d = \frac{K_H+K}{m_H C_H}$, we obtain the expressions for the parameters $\lambda_1$and λ_2 as follows,

$$\lambda_{1,2} = \frac{-(a+d) \pm \sqrt{(a+d)^2 - 4(ad-cb)}}{2} \tag{3.33}$$

Replacing the elements of the matrix A for their corresponding system parameters dependency we finally obtain:

$$\lambda_1 = \frac{-\left(\frac{K+K_C}{m_C C_C} + \frac{K_H+K}{m_H C_H}\right) + \sqrt{\left(\frac{K+K_C}{m_C C_C} + \frac{K_H+K}{m_H C_H}\right)^2 - 4\left(\frac{K+K_C}{m_C C_C}\frac{K_H+K}{m_H C_H} - \frac{K}{m_H C_H}\frac{K}{m_C C_C}\right)}}{2} \tag{3.34}$$

$$\lambda_2 = \frac{-\left(\frac{K+K_C}{m_C C_C} + \frac{K_H+K}{m_H C_H}\right) - \sqrt{\left(\frac{K+K_C}{m_C C_C} + \frac{K_H+K}{m_H C_H}\right)^2 - 4\left(\frac{K+K_C}{m_C C_C}\frac{K_H+K}{m_H C_H} - \frac{K}{m_H C_H}\frac{K}{m_C C_C}\right)}}{2} \tag{3.35}$$

3.3. NUMERICAL SIMULATOR

Using the equations (3.23) and (3.24) it was developed a numerical simulator of a thermal model for a temperature controlled semiconductor laser with tunable parameters using MATLAB/SIMULINK.

The simulator will enable a deep study on all the external influences swaying the temperature on a semiconductor laser package and therefore influencing its performance. Parameters like the environmental temperature, seebeck coefficient (different TEC performances) and thermal conductivity (different heat sinks) can be controlled so that the designer of the system can evaluate the best solution when implementing thermoelectric modules into semiconductor laser packaging.

Table 1 Values used on the simulation for the coefficients of the thermal model of the semiconductor laser and its thermoelectric cooler

$\alpha\ [VK^{-1}]$	$K\ [WK^{-1}]$	$K_H\ [WK^{-1}]$	$K_C\ [WK^{-1}]$	$C_C\ [J\ K^{-1}]$	$C_H\ [J\ K^{-1}]$
0.0137	0.0483	0.1609	0.0106	0.1871	1.3218

Using the testing set of parameters represented in Table 1, the temperature in steady state over the current applied on the thermoelectric cooler for the hot and cold side with an environmental temperature T_0 of $25ºC$ and a laser power of $P_l = 1W$ obtained through simulation is represented in Figure 3.4.

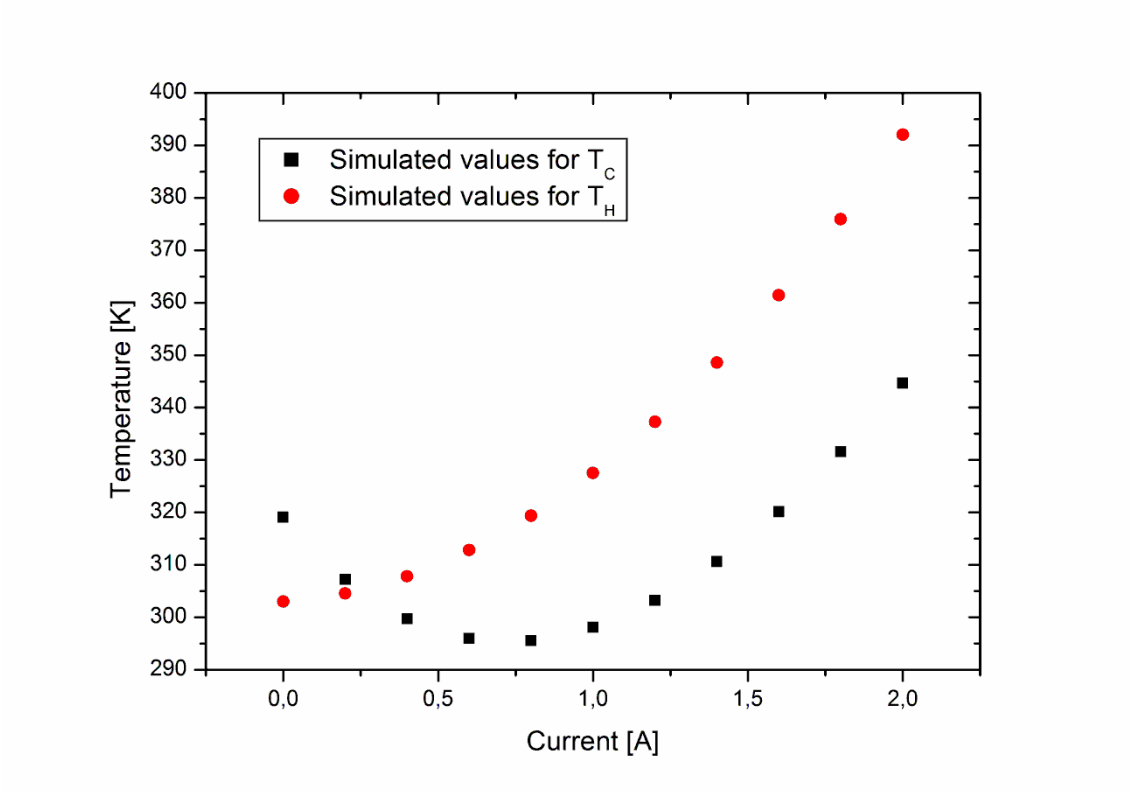

Figure 3.4 Temperature simulated for the cold and hot side over the current applied on the thermoelectric cooler for a laser power of 1W.

Let us now consider a current step applied to the peltier cooler, I_p, with an initial value of $0A$ and final value of $0.5A$ for a step time of $250s$, an environmental temperature T_0 of $25ºC$ and a laser power of $P_l = 1W$. The temperature variation with time obtained in simulation for the cold and hot side in Figure 3.5.

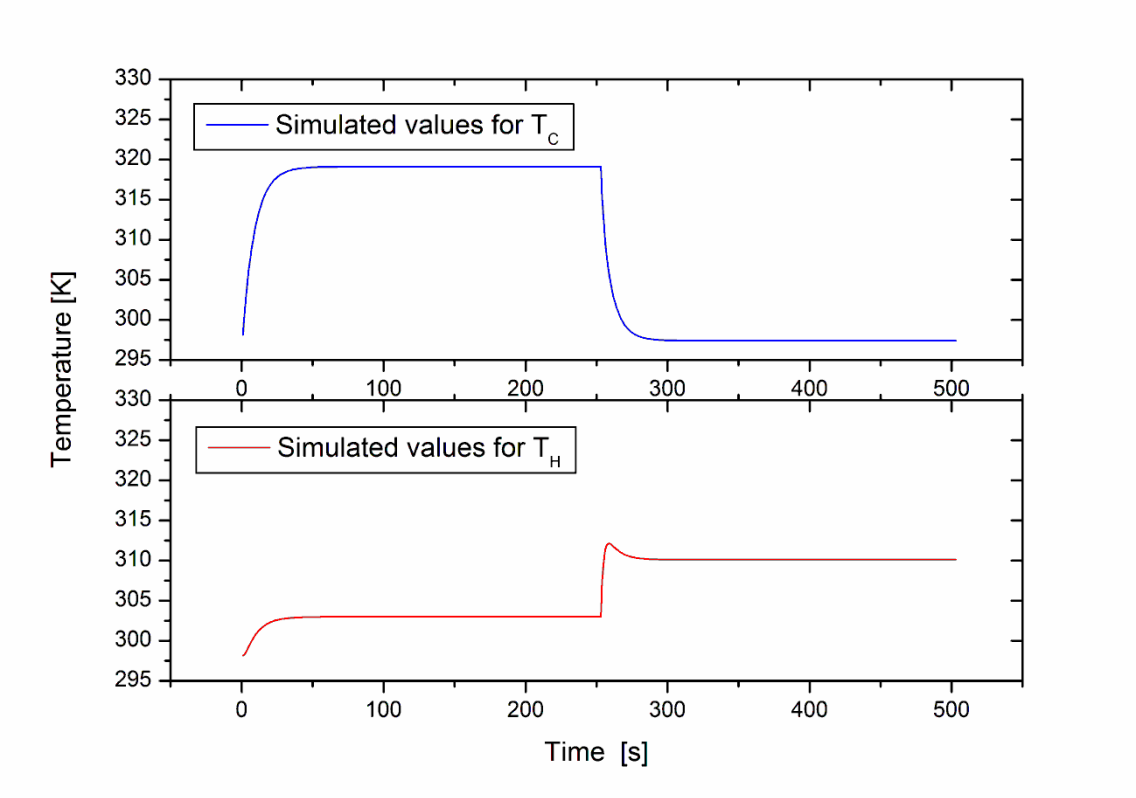

Figure 3.5 Temperature variation with time obtained in simulation for the cold and hot side for a current step applied to the peltier cooler with an initial value of $0A$ and final value of $0.5A$ for a step time of $250s$

Considering now the case with a current step applied to the peltier cooler I_p with an initial value of $0.5A$ and final value of $0A$ for a step time of $250s$, an environmental temperature T_0 of $25ºC$ and a laser power of $P_l = 1W$. The temperature variation with time obtained in simulation for the cold and hot side in Figure 3.6.

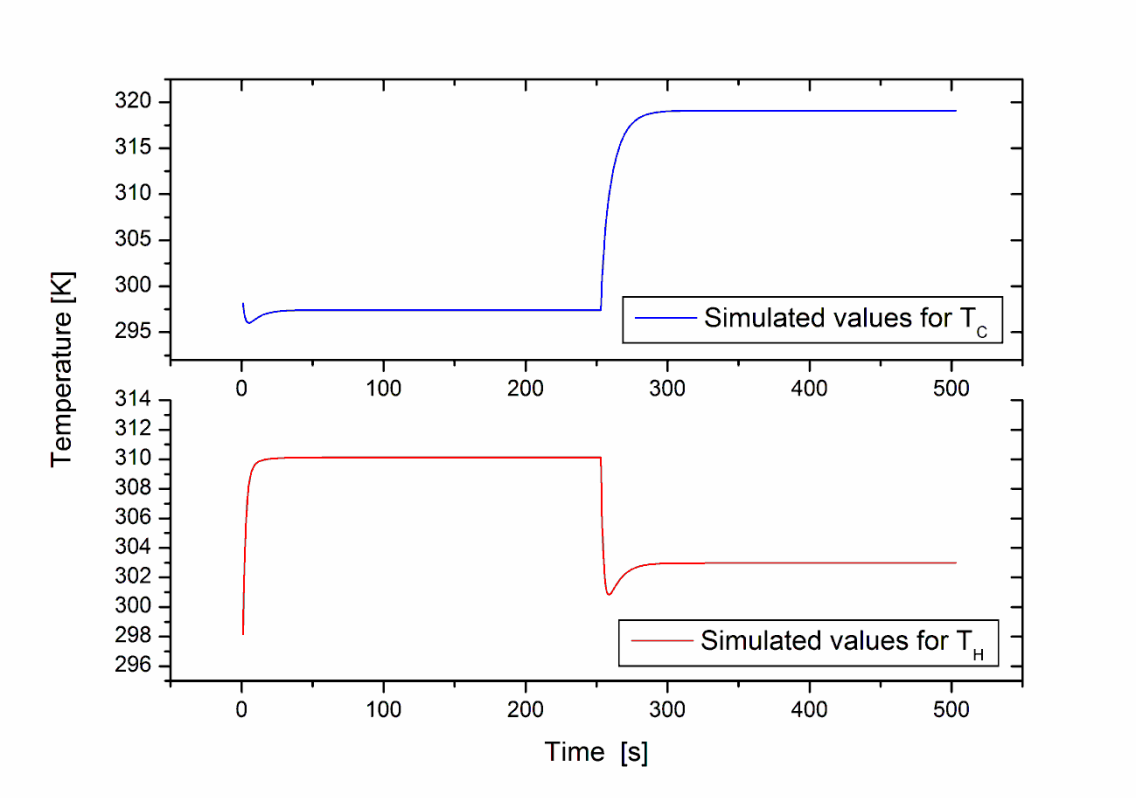

Figure 3.6 Temperature variation with time obtained in simulation for the cold and hot side for a current step applied to the peltier cooler with an initial value of $0.5A$ and final value of $0A$ for a step time of $250s$

While the simulator allows the designer to test and access different elements on the system, the lack of information provided regarding the material properties by the manufacturers makes it impossible applying direct theoretical means of predicting the performances of these modules. In the next chapters it will be exposed the approach of obtaining such parameters through minimization tools.

4. STUDY OF LASER PERFORMANCE TEMPERATURE DEPENDENCE

To verify the already previously stated need for an efficient laser temperature control, an experiment was made using a temperature controlled laser that had a thermoelectric cooler aggregated so that the temperature was easily set at the desired value. The laser used was module type FU-68SDF-V802MxxB a MQW DFB-LD module with single-mode optical fiber pigtail with a built-in thermoelectric cooler in a butterfly package [38].

This experiment was done so that we could verify the dependency of the semiconductor laser's optical power to its temperature. To test the average power in the optical fiber it was used a power meter.

The output optical power versus the pump current curve was then obtained using the data collected for the temperatures of 15ºC, 25ºC, 35ºC and 45ºC through a linear approximation in both of its functioning modes, spontaneous emission and stimulated radiation, of the measured data from the optical power for different values of the input current of the laser for each of the temperatures. The curves obtained for the acquired data are represented in Figure 4.1.

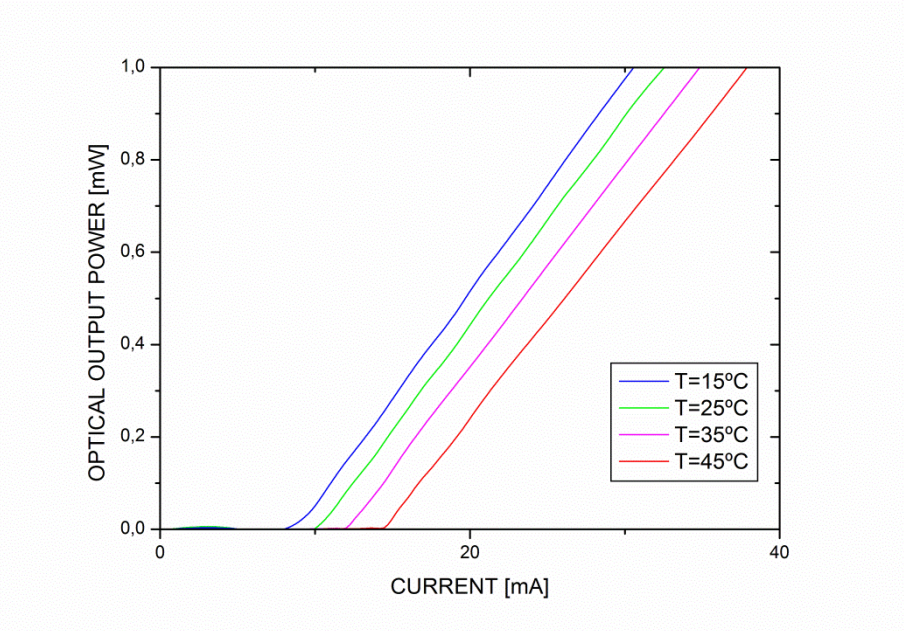

Figure 4.1 Semiconductor laser output power versus current for different temperatures

The equation for output optical power versus the injected current in the stimulated emission region is of the form:

$$y = C_1 x + C_2 \tag{4.1}$$

The slope of the line obtained for the stimulated emission is representative of the laser's efficiency. As previously stated, the larger its slope and the closer the starting point of the curve is to the origin, the better is the laser diode as the output optical power is higher for smaller currents injected on the laser.

To obtain the threshold current of the laser and its efficiency it was used a fitted linear regression model to the data related to the stimulated emission of the laser (Figure 4.2).

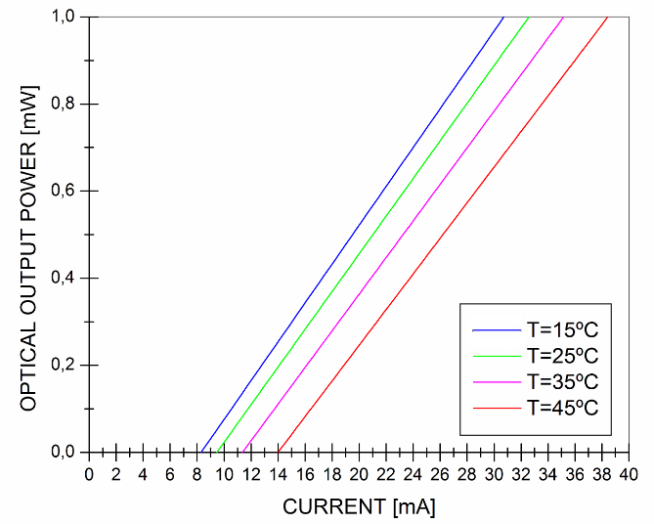

Figure 4.2 Linear fit of the stimulated emission optical power output of a semiconductor laser for different temperatures

The slop of the fitted curve, represents the efficiency of the laser and the threshold current, the point when the laser first demonstrates stimulated emission, can be obtained through:

$$I_{th} = -\frac{C_2}{C_1} \tag{4.2}$$

In the next table it's represented the results obtained for the efficiency and threshold current of the laser for the tested temperatures.

Table 2 Values of the efficiency and threshold current obtained based on the linear fit of the laser's optical output power

TEMPERATURE [ºC]	EFFICIENCY [mW/mA]	THRESHOLD CURRENT [mA]
15	$0{,}04458 \pm 6{,}61 \times 10^{-5}$	$8.391 \pm 0{,}00368$
25	$0{,}04326 \pm 1{,}22 \times 10^{-4}$	$9.571 \pm 0{,}00645$
35	$0{,}04164 \pm 1{,}68 \times 10^{-4}$	$11.043 \pm 0{,}01093$
45	$0{,}04053 \pm 1{,}33 \times 10^{-4}$	$13.773 \pm 0{,}00868$

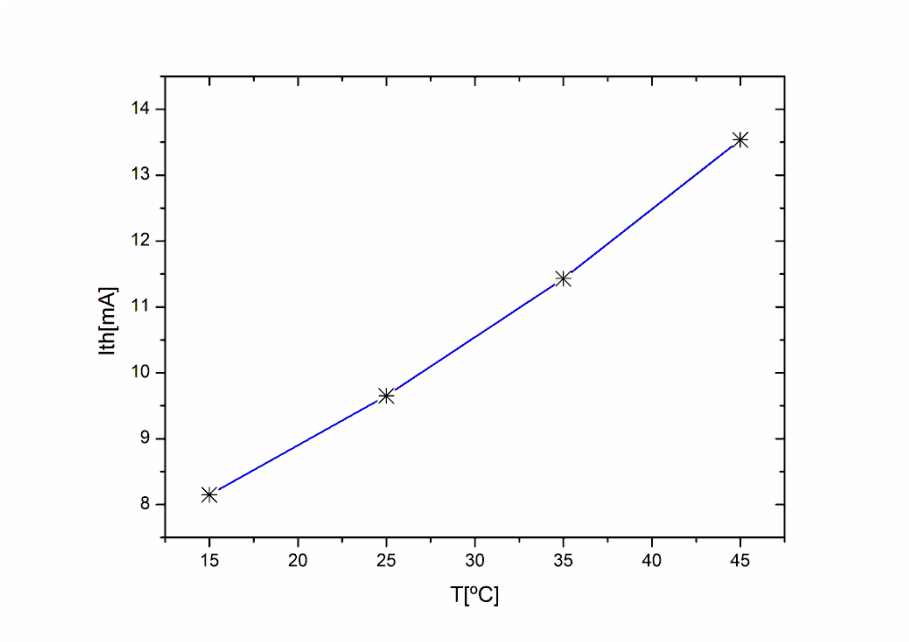

Figure 4.3 Threshold current increase with temperature

The values obtained go in agreement with the fact that the laser behavior is temperature dependent. Not only can we verify a decrease in efficiency and extinction ratio with the temperature rise but also an increase of the threshold current (Figure 4.3). This means that for the same injected current the laser's optical output power will be inferior for greater temperatures of the device, which has clear consequences. This reinforces the idea for the need to control the temperature of the laser package.

5. PELTIER MODULE PARAMETER ASSESSMENT

To test the thermal model for the peltier module and its parameters extraction accuracy it was considered the simplified model represented in Figure 5.1 so that the hot side of the system will be united into one component. This allowed us while adding an extra component to the system to consider only one temperature for the set hot junction and heat sink and measure it against the junction of the two elements. To do so, the temperature T_H, thermal conductivity K_H, mass m_H and heat capacity c_H will refer to the set heat sink and hot junction of the peltier module:

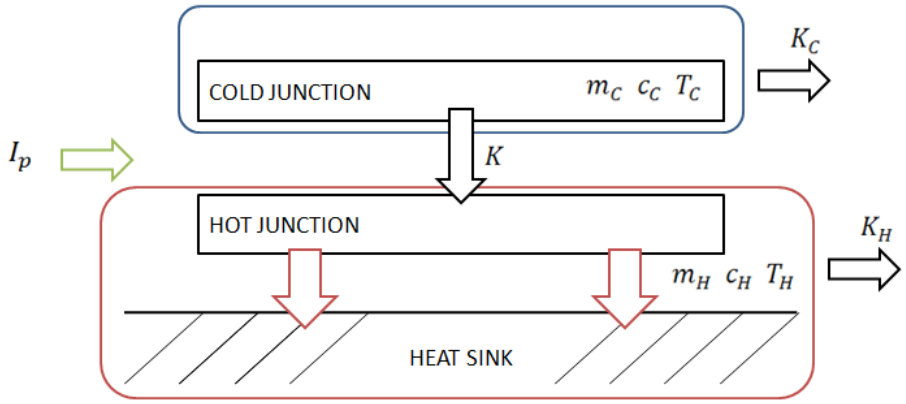

Figure 5.1 Simplified thermal model for the peltier element with a heat sink

To test the thermal model in Figure 5.1 the experiment represented in Figure 5.2 was made. This experiment allowed us to measure the temperature in the two sides of the peltier module for different currents applied. To do so, a thermistor was placed against each side of the peltier module using a thermal paste to maximize the heat transfer and eliminate possible air gaps between the thermistor and the device.

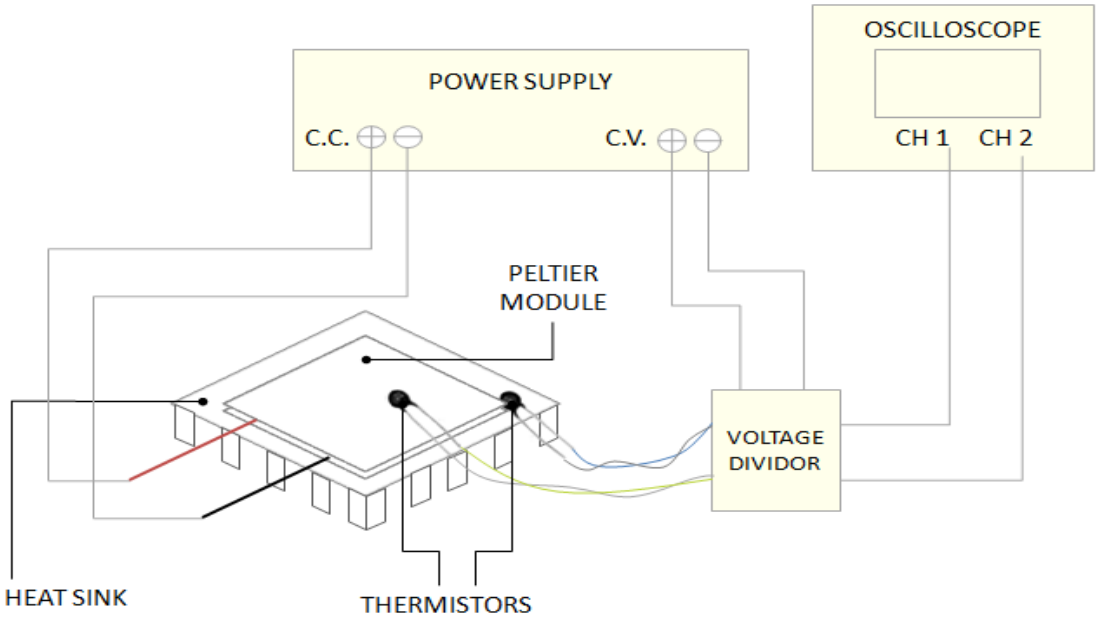

Figure 5.2 Experimental setup of a peltier module with a heat sink to determine the coeficcients that describe the heat model

A thermistor is a resistor thermally sensible that exhibits a difference in resistance with the temperature change. The thermistors used were beaded 10K Negative Temperature Coefficient (NTC) thermistors.

In order to interpret the temperature measured by both the thermistors it was used voltage dividers as represented in Figure 5.3. Each thermistor is connected in series with a known resistor to form a voltage divider and a known voltage that is applied across the divider. The oscilloscope is then connected to the center of each one of the voltage dividers so that it was possible to measure the output voltages.

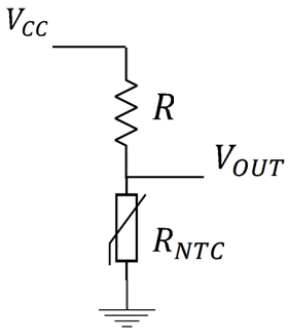

Figure 5.3 Thermistor circuit - Voltage divider

The thermistor R_{NTC} is given by the equation:

$$V_{OUT} = \frac{R_{NTC}}{R + R_{NTC}} V_{CC} \tag{5.1}$$

where V_{CC} is the known voltage applied, R a known resistor and V_{OUT} the output voltage.

NTC Thermistors are non-linear resistors, which alter their resistance characteristics with temperature. The resistance of a NTC thermistor will decrease as the temperature increases. They have the advantage of a very high sensitivity to temperature changes, but the disadvantage of an aggressively nonlinear characteristic. The early scientific literature regarding the resistance versus temperature relationship for NTC thermistors proposed the assumption that these materials followed the model in conductivity physics known as intrinsic conduction. However, with the improvements in technology for temperature calibration, the early expression, known as the Beta Equation, was found to be inadequate for applications requiring more precise temperature measurement. In their search for an empirical expression that provided relatively accurate interpolation of the resistance/temperature characteristic in the oceanographic temperature range of -2°C to 35°C, Steinhart and Hart investigated the curve fitting capability of:

$$\frac{1}{T} = A + Bln(R_{NTC}) + Cln(R_{NTC})^2 + Dln(R_{NTC})^3 \tag{5.2}$$

and later discovered that by eliminating the squared term, the following equation:

$$\frac{1}{T} = A + Bln(R_{NTC}) + Dln(R_{NTC})^3 \tag{5.3}$$

improved the curve fitting results for the ocean water temperatures they were studying. This equation became known as the Steinhart-Hart Equation and it was used to find the temperature relationship with the resistance measured of the thermistor for this experiment. A, B and C are the Steinhart–Hart coefficients which vary depending on the type and model of thermistor and the temperature range of interest. The values used for these coefficients were:

Table 3 Values used for the Steinhart–Hart coefficients

$\boldsymbol{A}$	$\boldsymbol{1,14 \times 10^{-3}}$
$\boldsymbol{B}$	$2{,}32 \times 10^{-4}$
$\boldsymbol{C}$	$9{,}49 \times 10^{-8}$

Using the experimental procedure described previously, the voltages measured in the voltage divider output with the oscilloscope for both the cold and hot side were collected for currents between 0 and 1,6A with an interval of 0,1A.

Between each measurement it was given some time to stabilize the voltage measured in both sides so that we could after refer the data collected to the simplified steady-state model for the peltier module. The voltages collected were then converted into their corresponding resistance using equation (5.1). Finally these resistances, measured in both sides of the peltier module, for each of the considered currents, were applied to equation (5.3) to obtain the equivalent temperature. Figure 5.4 contains the data obtained using this procedure for both the hot and cold sides of the module.

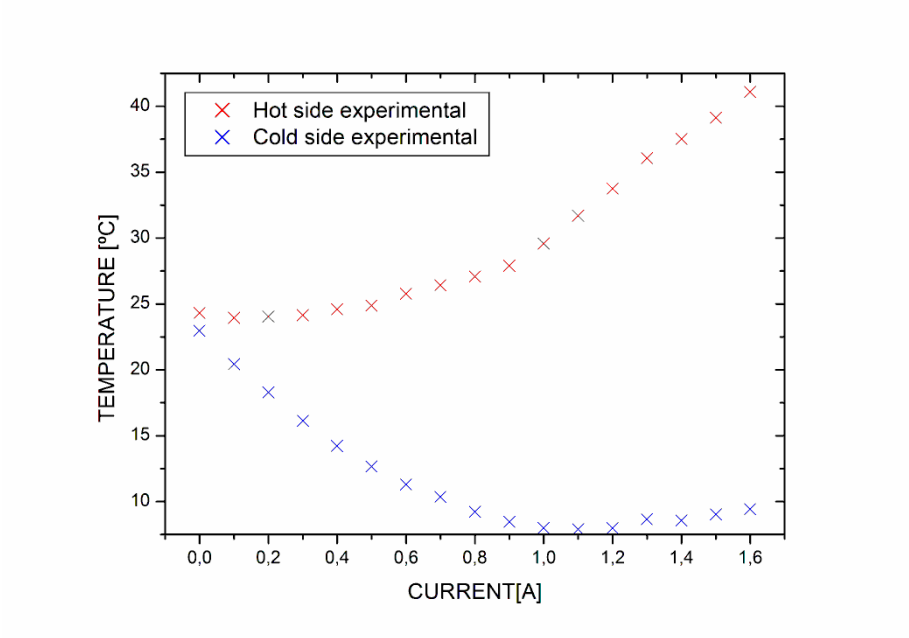

Figure 5.4 Temperature variation with current applied to the peltier module measured using the experimental setup from Figure 5.2

Examining the obtained data it's possible to see that by increasing the current applied to the peltier module the temperature difference between both sides increases, with the temperature on the hot side increasing and the temperature on the cold side decreasing initially. As the current applied begins to increase to higher values, the temperature on the cold side will begin to revert and start to increase. This means that the Joule heating and thermal conduction term weight will surpass the peltier effect.

To determine the parameters that described this system the temperature was measured over time for a set of initial currents applied to the peltier module. This procedure consisted on, for a given current applied to the peltier module, it was allowed enough time to let the temperature stabilize, choosing the temperature on the cold side as a reference for this experiment. When the system was in steady state, the current supply would be switch off. For each one of the

initial current applied the temperature on the cold side was collected over time until it stabilized to room temperature. Data values collected from this experiment over time of the cold side described an exponential growth like it was predicted by equation (3.15) and it's represented in Figure 5.5 for an initial current applied of $I_p = 0.5A$ (top), for an initial current of $I_p = 1A$ (middle) and for an initial current of $I_p = 1A$ (bottom).

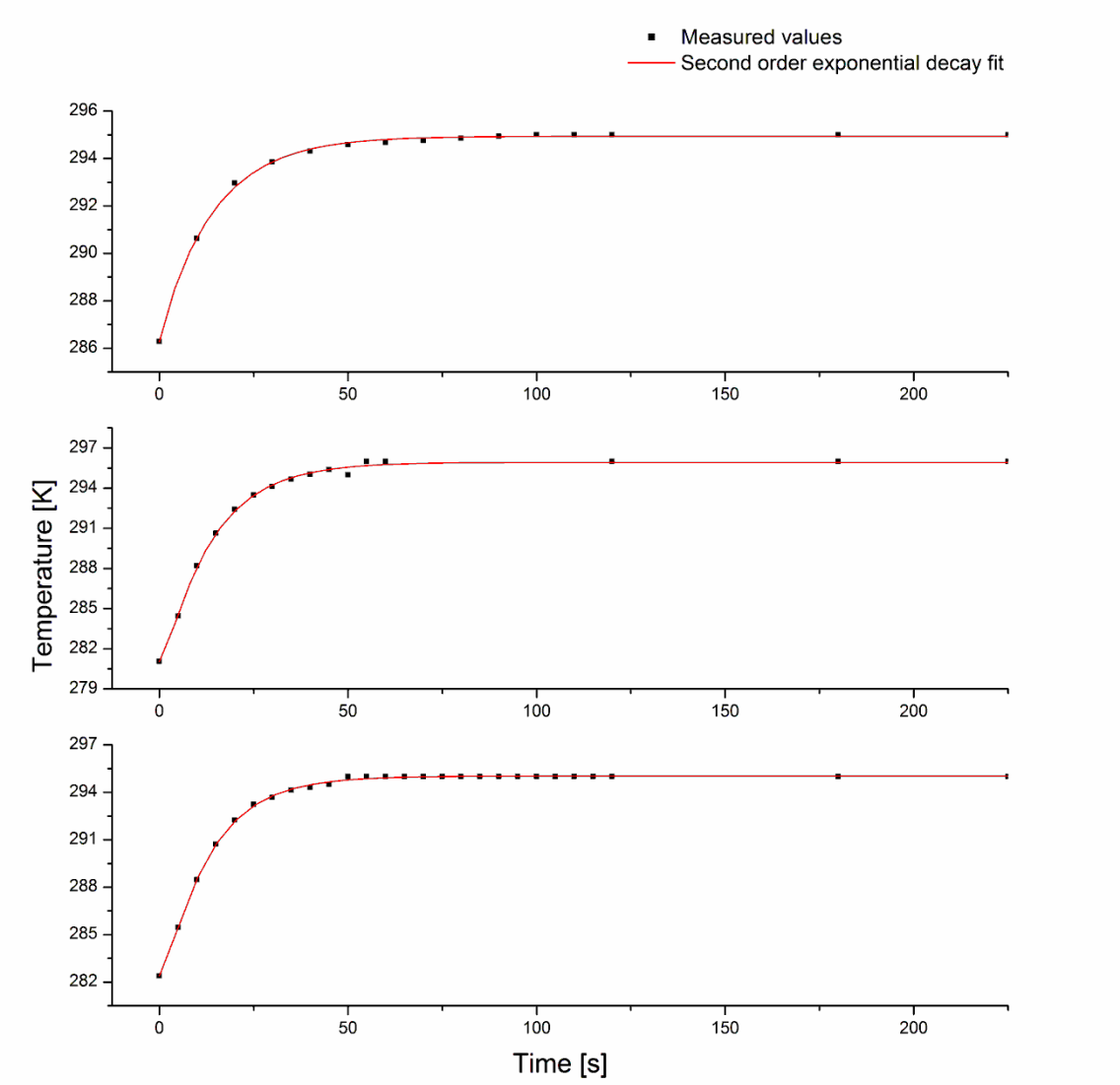

Figure 5.5 Second order exponential fit for the temperature of the pletier's module cold side after the switch off of the current supply of $I_p = 0.5A$ (top), $I_p = 1A$ (middle) and $I_p = 0.8A$ (bottom)

For each one of the experiments it was made the non-linear second order exponential decay fit for the equation:

$$y = y_0 + A_1 e^{-\frac{x}{t_1}} + A_2 e^{-\frac{x}{t_2}} \tag{5.4}$$

The parameter y_0 represents the system's environment temperature. Variables t_1 and t_2 represent the exponential time constants of the system and depend on the thermal conductance between each of the elements and their mass specific heat capacity and relate to the equations (3.17) and (3.18) through the equation:

$$t_{1,2} = \frac{1}{\lambda_{1,2}} \tag{5.5}$$

The values of each one of the variables obtained from the curve fitting of the previous equation are expressed in Table 4.

Table 4 Second order exponential fit parameters for the temperature of the pletier's module cold side after the switch off of different current supplies

$I_p\ [A]$	y_0	A_1	$t_1[s]$	A_2	$t_2[s]$
0.5	294.936 ±0.038	-8.41 ±1.74	14.62 ±1.78	-0.24 ±1.76	3.345 ±4.59
0.8	295.019 ±0.021	-15.00 ±0.66	12.06 ±0.37	2.36 ±0.67	2.570 ±1.03
1	295.92 ±0.12	-16.75 ±1.07	13.067 ±0.90	1.884 ±1.16	2.123 ±3.19

The values obtained for the exponential time constants of the system for all the experiments were reasonably identical as it was expected. Their average value was used to simulate the system together with the set of values expressed in Figure 5.4.

In order to find the unknown parameters that describe the system α, K, K_H, K_C, C_C and C_H it was used the nonlinear programming solver fmincon in MATLAB that finds the minimum of a constrained nonlinear multivariable function. To set the optimization options it was used the function optimset to create optimization options structure that limited the iterations. The function used in the minimizing function was the normalized mean square error:

$$NMSE = \left|\left|\frac{(x-y)^2}{x}\right|\right| \tag{5.6}$$

where y is a prediction of the measured values x.

The measured values x combine the set values of the temperatures measured in the cold and hot sides, $T_C$and T_H, represented in Figure 5.4 and λ_1 and λ_2, the reciprocal average of the values obtained for the exponential time constants, t_1 and t_2, of the system represented in Figure 5.4.

The prediction of the measured values for the temperatures measured in the cold and hot sides, $T_C$and T_H were obtained through equations (3.8) and (3.9) and parameters λ_1 and λ_2 through equations (3.17) and (3.18).

The values for the unknown parameters that describe the system that were obtained in the MATLAB script for a normalized mean square error of 0.0471 were:

Table 5 Values obtained for the coefficients after minimization

$\boldsymbol{\alpha}$ $[\boldsymbol{VK^{-1}}]$	$\boldsymbol{K}$ $[\mathbf{WK^{-1}}]$	$\boldsymbol{K_H}$ $[\mathbf{WK^{-1}}]$	$\boldsymbol{K_C}$ $[\mathbf{WK^{-1}}]$	$\boldsymbol{C_C}$ $[\mathbf{J\,K^{-1}}]$	$\boldsymbol{C_H}$ $[\mathbf{J\,K^{-1}}]$
$\mathbf{0.8291}$	0.0246	3.3854	0.3908	5.8117	47.7133

The value obtained for the thermal conductivity K_H is superior to the value of K_C due to the implementation of a heat sink to the system. This will increase the thermal conductivity of the hot side of the peltier element improving the dissipation of the heat generated from the device by maximizing its surface area in contact with the cooling medium surrounding it, in this case the air. The fact that C_H represents the heat capacity of the hot side of the peltier module combined with the heat sink increases his value as it depends not only of the to the mass specific heat capacity c_m, an intrinsic characteristic of a particular substance but also of its mass as demonstrated by equation (3.5).

The values obtained through the described MATLAB script were used in equations (3.12) and (3.11) for the set of values of current applied to the peltier module used in the experimental setup for the temperature variation with current applied to the peltier module expressed in Figure 5.4. The results obtained are represented in Figure 5.6.

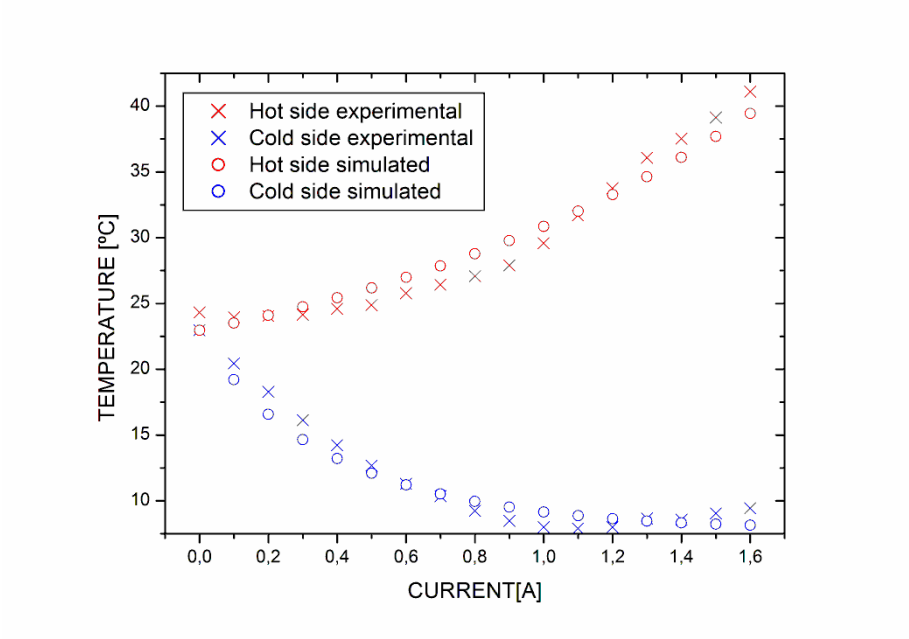

Figure 5.6 Experimental and simulated values for the temperature variation in with current applied to the peltier module

6. LASER DIODE WITH THERMOELECTRIC COOLER CARACTERIZATION

To understand the optimized function of each system is fundamental to determine each of the parameters of the thermal model that describes it. As it was previously demonstrated, some of these parameters are easily controlled and determined with simple measurements.

The experimental procedures took place in *Coriant* using laser boards from commercial optical communication systems. The laser used in the experimental procedures was a laser in a 14-pin butterfly package consisting of a laser diode, thermoelectric cooler, and a monitor diode [39] with an output power versus input current curve represented in Figure 6.1. The environment temperature was set and controlled with the use of an oven. The measurement of the temperature on the hot side was made using a thermocouple attached to the laser package, or to the heat sink if applicable, with thermal paste and tape. The measurement of the temperature on the laser was made using the thermistor inside the laser package.

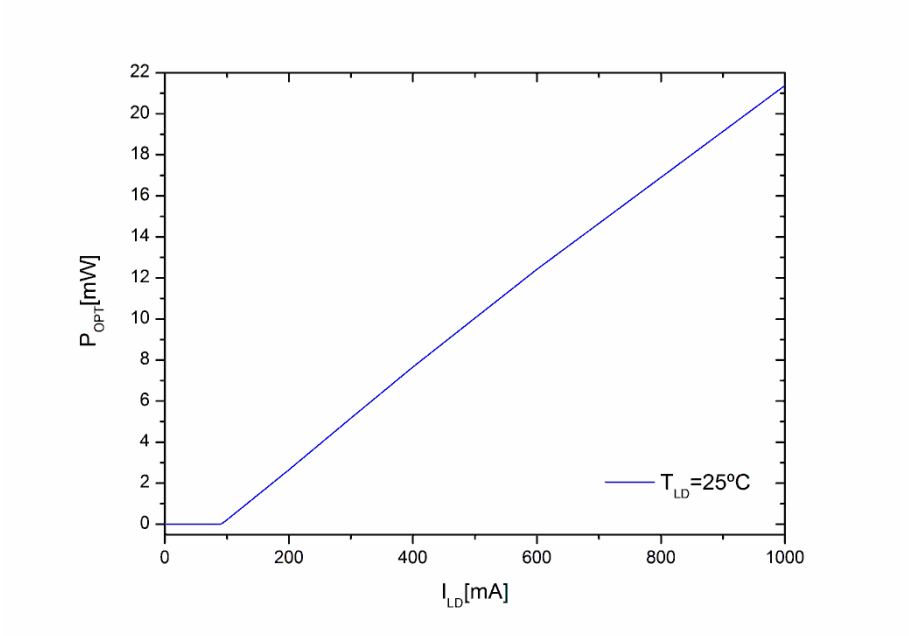

Figure 6.1 Laser diode output power versus input current curve

To analyze the effect of the laser's addiction to the previous system it was made an experiment to observe its influence on its behavior. In Figure 6.2 it's represented the temperature measured outside the package T_H and the temperature measured in the laser inside the package T_C along an increasing current applied on the thermoelectric cooler for different currents injected to the laser diode I_{LD}.

Observing the curves obtained we can verify that the laser diode will affect the temperatures that describe the system by shifting the curves up with an approximately constant increase of the temperature. If we were to set the temperature of the laser to 25ºC to stabilize its performance we would need a higher current applied to the thermoelectric cooler for higher currents applied to the laser. We can then conclude that for a higher power required in the laser diode, the more current needs to be applied to stabilize the temperature to the aimed value.

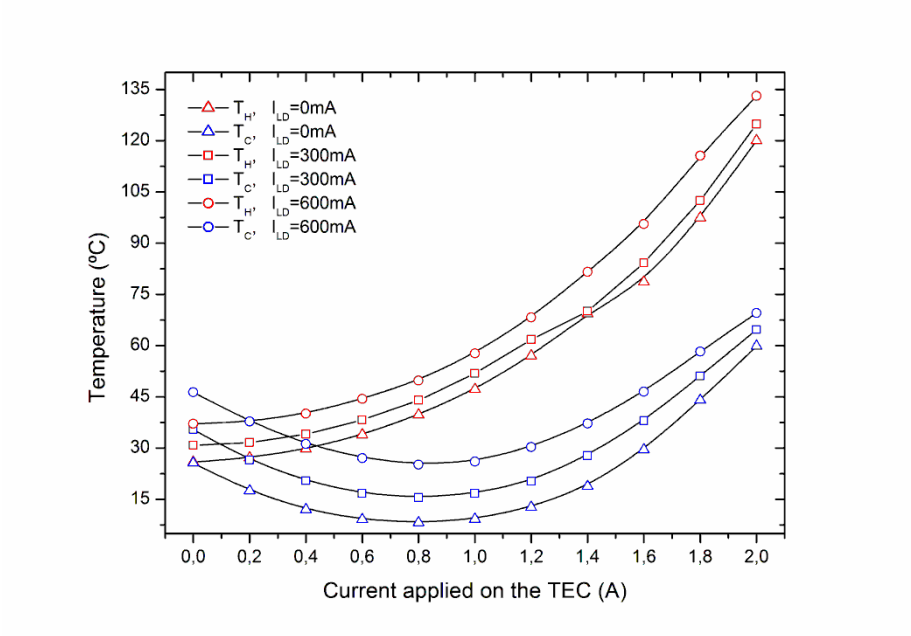

Figure 6.2 Temperature over the current applied on the thermoelectric cooler for different values of current applied to the laser diode

The environmental temperature can be controlled in the laboratory with the use of a temperature controlled oven. In order to see the effect of the change of the environmental temperature the oven was set for temperature of 30ºC and 50ºC, at each point the temperature was measured on the heat sink attached to the laser package and in the laser. The results obtained are shown in Figure 6.3.

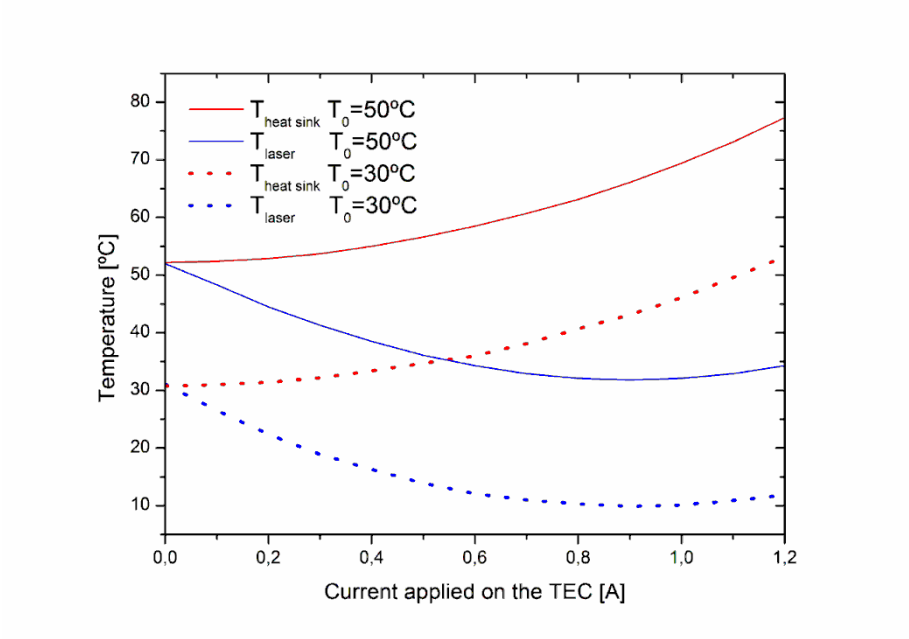

Figure 6.3 Effect of the environmental temperature difference on the temperature on the laser diode for different currents applied on the thermoelectric cooler

By altering the environmental temperature there is a shift on the corresponding temperature of the each part of the system approximately on the difference created. There is a slight increase on the temperature difference for higher currents applied however it's possible to make an estimate on the behavior of the system for different environmental temperatures.

The environmental temperature is easily controlled in a laboratory controlled ambient but it can't normally be the answer to create a more efficient system. The system should be able to control the temperature of the laser diode facing the environmental temperature presented or for one specified. To do so, the thermoelectric cooler must draw enough heat from the laser so that it can work on a constant desirable temperature for that specific ambient temperature.

While normally the answer to reduce the temperature on the laser diode is to apply current to the thermoelectric cooler until the desired temperature is achieved, the fact that there is not a linear relation between the current applied to the thermoelectric cooler and the temperature obtained obliges a more in-depth study of the system.

Figure 6.4 represents the temperature measured on the laser diode for increasing values of current applied to the thermoelectric cooler. The values obtained were measured for an ambient temperature of 30ºC set in the oven.

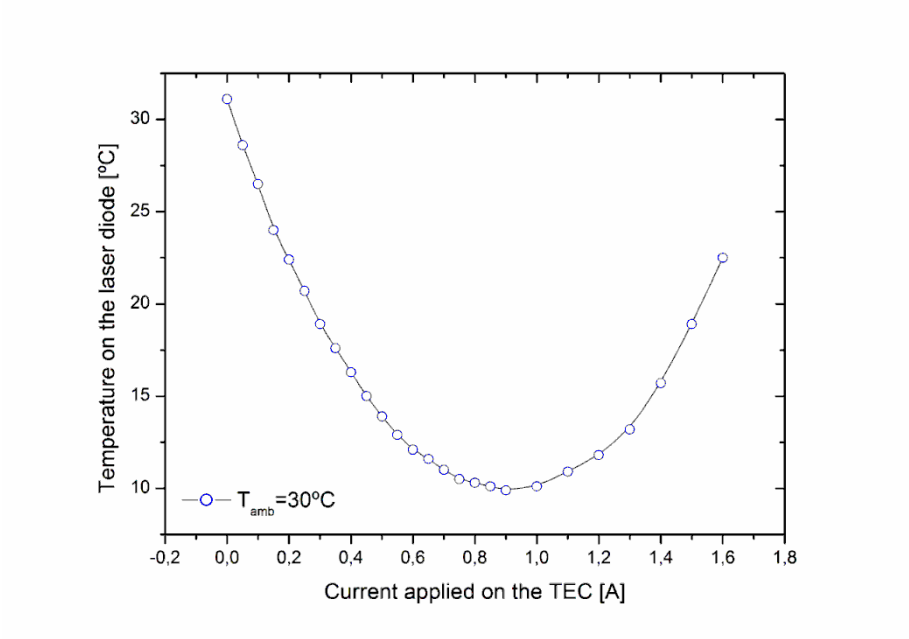

Figure 6.4 Temperature on the laser diode for different currents applied on the thermoelectric cooler with an environmental temperature of 30ºC

Observing the curve that describes the behavior of the temperature we can see that there is a point where the temperature will cease to decrease and instead start increasing. This behavior can be predicted by the equation (3.23). As the current applied begins to increase to higher values, the temperature on the laser will begin to revert and start to increase meaning that the Joule heating and thermal conduction term weight will surpass the peltier effect.

While there is no way to reduce the Joule heating without decreasing the current applied to the thermoelectric cooler, the weight of the thermal conduction term depends on the temperature difference between the laser and the surroundings namely the temperature of the hot side. By decreasing the temperature on the hot side the influence on the temperature of the laser of the parameter referring to the thermal conduction between the laser and the hot part of the system will diminish. To solve the problem of an increasing heat transfer from the hot side of the thermoelectric cooler to the laser a heat sink can be attached to the laser package. By adding a heat sink or replacing the existing heat sink for one with a better performance the thermal conductivity with the surrounding will increase making the temperature decrease.

In order to understand the effect of the performance improvement of a heat sink on the system it was made the same experiment in the identical environmental condition attaching two different heat sinks to the laser package where heat sink number 2 was a bigger and more efficient heat sink than heat sink number 1.

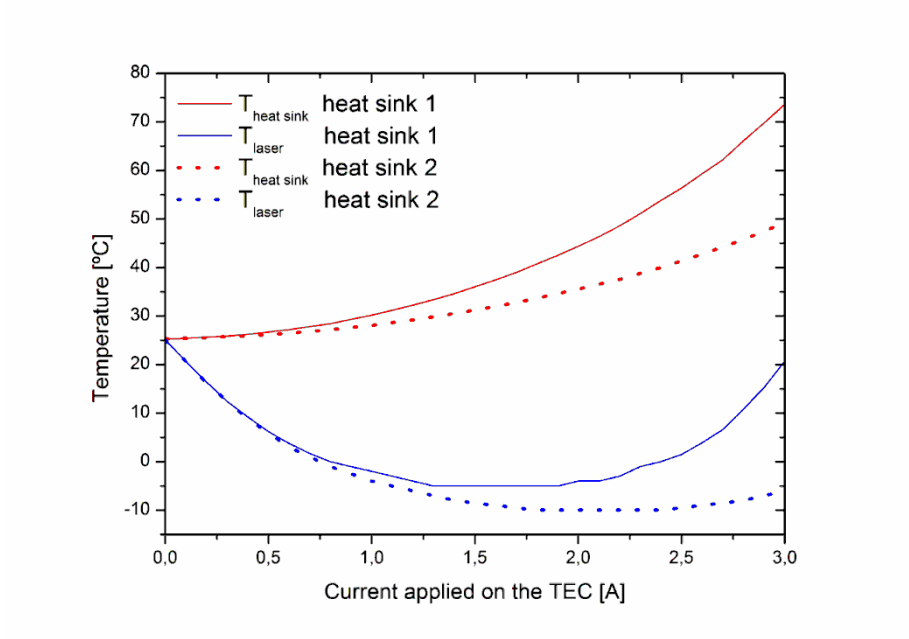

Figure 6.5 Temperature on the laser diode for different currents applied on the thermoelectric cooler for two different heat sinks attached to the laser package

Analyzing Figure 6.5 we can verify that the heat sink with better performance (heat sink 2) enabled the temperature on the cold side to reach lower temperatures while also allowing a more controlled response to a higher current applied. By improving the heat transfer from the laser package to the surroundings the laser was able to reach lower temperatures even for higher currents.

The effect of a better heat sinking solution will completely alter the behavior of the temperature curve over current applied on the thermoelectric cooler of the system. This makes analyzing the behavior of a system with a different heat sink solution less straightforward than altering other elements as the environmental temperature or current applied to the laser. While its effect on the system can be less obvious than other elements, using an accurate thermal model can precisely describe the system just by altering its thermal conductivity value K_H on equation (3.24). This value can be provided by the manufacturer or by a series of experimental tests to determine the parameters of the system. There are a lot of factors to take into account when considering this type of system, from the environment temperature it should be working in to the chosen heat sinking solution but with a thermal model that accurately represent all this parameters the designer of the system can make the decisions for a better performance.

To identify the exponential time constants of the second order exponential decay that described the system, the temperature was measured over time, injecting and switching off a set of currents applied on the thermoelectric cooler for the system on steady state. For each one of the currents applied on the thermoelectric cooler, the temperature against the heat sink

attached on to the laser package was collected over time until it stabilized to room temperature. The values collected from this experiment are represented in Figure 6.6.

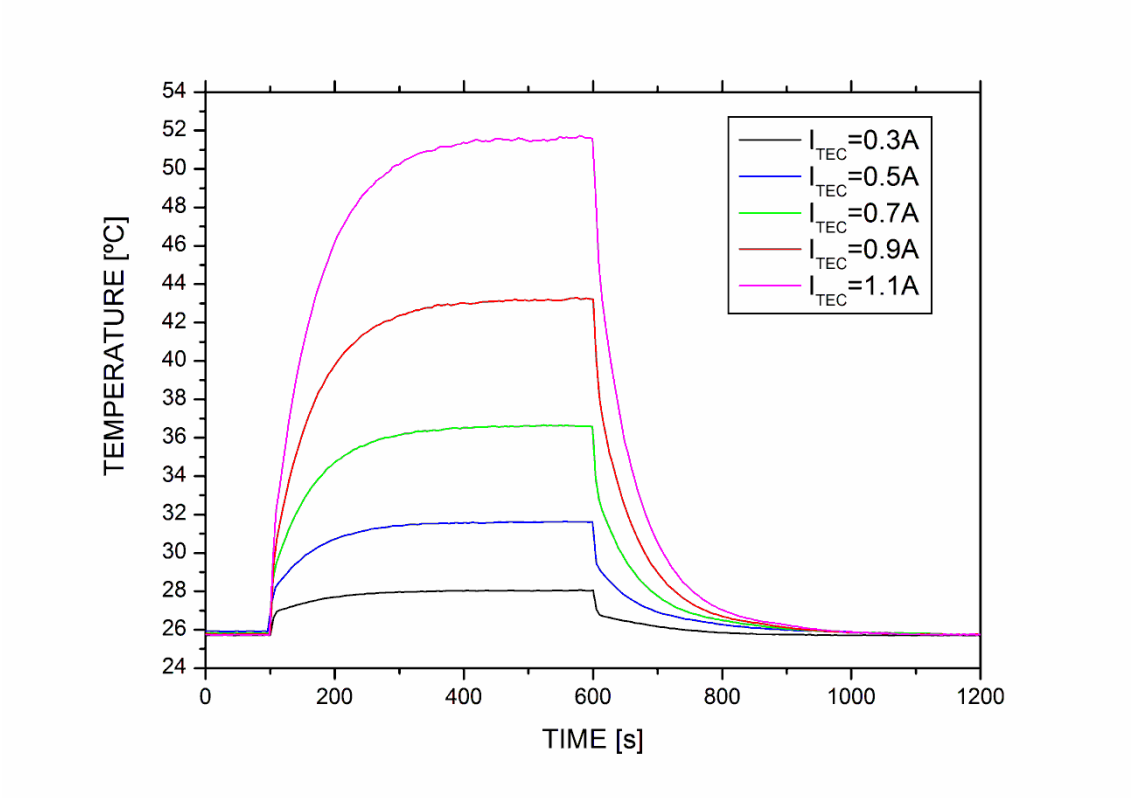

Figure 6.6 Temperature on the heat sink attached to the laser package over the injection and switch off of current applied on the thermoelectric cooler

Like previously the temperature was measured over time but this time for a set of initial currents applied to the thermoelectric cooler. This time the method consisted on allowing enough time to let the temperature stabilize for a given current applied to the thermoelectric cooler using the temperature on the laser diode as the reference. When the system reached a steady state a current on the laser diode would be injected until it reached a new steady state. Then the current on the laser diode would be switched off. The temperature of the laser diode was collected over time until it stabilized to room temperature for each one of the initial currents applied on the thermoelectric cooler and on the laser. The values collected from this experiment over time of the cold side described an exponential decay when the current injected on the laser diode was switched off like it was predicted by equation (3.32) and are represented in Figure 6.7.

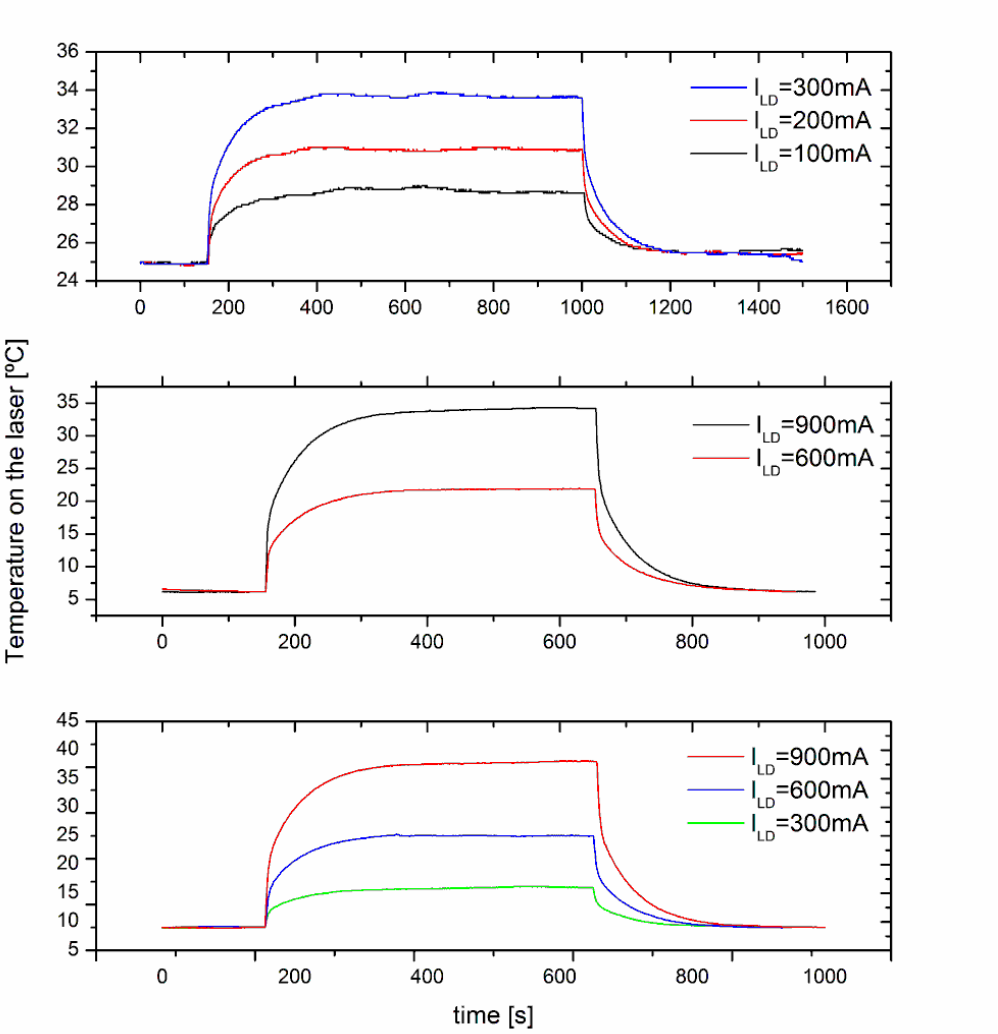

Figure 6.7 Temperature on the laser diode over the injection and switch off of current applied on the laser diode for $I_p = 0A$ (top), $I_p = 0.7A$ (middle) and $I_p = 0.5A$ (bottom)

For each one of the experiments it was made the non-linear second order exponential decay fit for the equation (5.4) where variables t_1 and t_2 represent the exponential time constants of the system and depend on the thermal conductance between each of the elements and their mass specific heat capacity and relate to the equations (3.17) and (3.18) through the equation (5.5).

The values of each one of the variables obtained from the curve fitting of the equation (5.4) are expressed in Table 6.

Table 6 Values obtained for the non-linear second order exponential decay fit of the curves represented in Figure 6.7

$I_p\ [A]$	$I_{LD}\ [mA]$	y_0	A_1	$t_1(s)$	A_2	$t_2(s)$
0	100	25.5528 ±0.0033	1.033 ±0.052	3.14 ±0.31	1.996 ±0.026	49.76 ±0.84
	150	25.4993 ±0.0045	1.332 ±0.071	2.74 ±0.29	2.808 ±0.033	50.24 ±0.79
	200	25.4400 ±0.0029	1.929 ±0.043	3.21 ±0.14	3.566 ±0.021	54.40 ±0.43
0.5	300	9.1489 ±0.0054	2.627 ±0.048	3.14 ±0.12	4.353 ±0.025	49.97 ±0.43
	600	8.8911 ±0.0096	7.017 ±0.068	4.163 ±0.082	9.817 ±0.038	58.20 ±0.36
	900	8.994 ±0.017	12.36 ±0.13	3.893 ±0.083	18.042 ±0.071	55.87 ±0.35
0.7	600	6.2261 ±0.0072	6.372 ±0.050	3.439 ±0.054	9.105 ±0.023	61.82 ±0.28
	900	6.2136 ±0.0091	11.569 ±0.071	3.288 ±0.041	16.990 ±0.034	55.94 ±0.19

Repeating the procedures used in chapter 0, the values for the unknown parameters that describe the system that were obtained in the MATLAB script for a normalized mean square error of 0.3689 are represented in Table 7.

Table 7 Values obtained for the coefficients of the thermal model of the semiconductor laser and its thermoelectric cooler after minimization for differents values of current applied to the laser

$\alpha\ [VK^{-1}]$	$K\ [\mathrm{WK^{-1}}]$	$K_H\ [\mathrm{WK^{-1}}]$	$K_C\ [\mathrm{WK^{-1}}]$	$C_C\ [\mathrm{J\,K^{-1}}]$	$C_H\ [\mathrm{J\,K^{-1}}]$
0.0137	0.0483	0.1609	0.0106	0.1871	8.3218

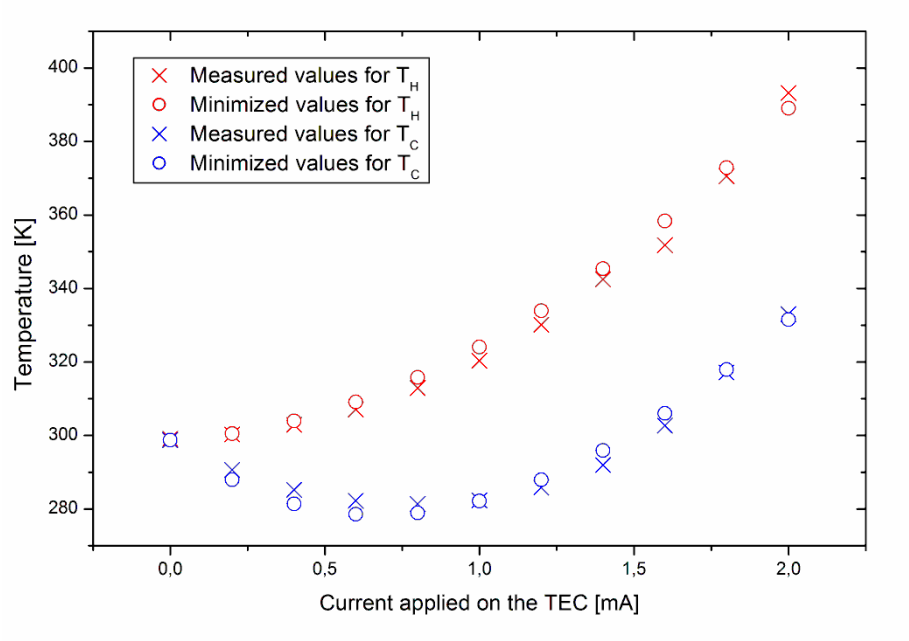

Figure 6.8 Temperature measured over the current applied on the thermoelectric cooler with the laser turned off and their respective values obtained using the parameters from Table 7

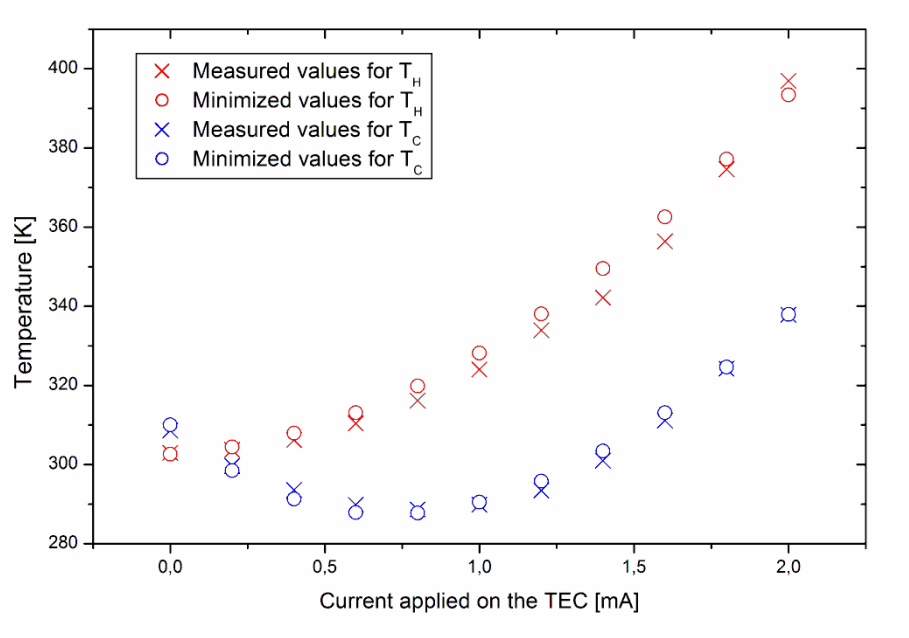

Figure 6.9 Temperature measured over the current applied on the thermoelectric cooler for a current applied on the laser of 300mA and their respective values obtained using the parameters from Table 7

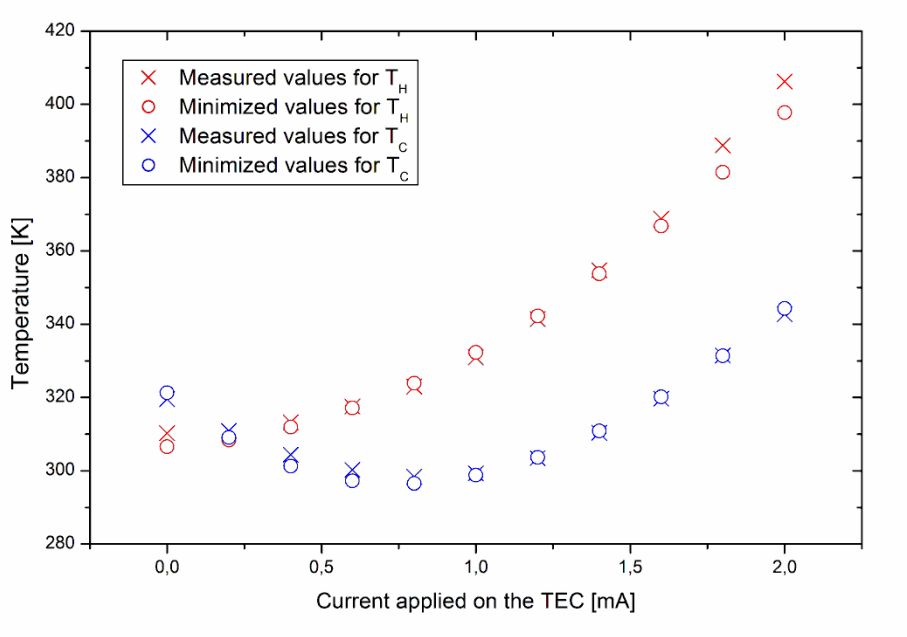

Figure 6.10 Temperature measured over the current applied on the thermoelectric cooler for a current applied on the laser of 600mA and their respective values obtained using the parameters from Table 7

The experimental values for the temperatures in both sides were well described by the analytical model having obtained similar values even for different currents applied to the semiconductor laser.

7. CONCLUSION

In this work it was created an approximate thermal model simulator using MATLAB/SIMULINK that enabled the study of the different factors that sway the temperature on a semiconductor laser package, therefore influencing its performance, as the environmental temperature, the heat sinking solution and the optical power of the laser used.

One of the main goals of this thesis was to provide designers, aiming to implement thermoelectric modules into semiconductor laser packaging, a method of evaluating the performance of a certain thermoelectric module. The lack or insufficiency of information provided regarding the material properties by the manufacturers made designers incapable of applying direct theoretical means of predicting the performances of these modules.

By using a simplified thermal model for the laser package system and laboratorial measurements along with minimizing techniques we were able to determine parameters that described the system that could be then used in the created simulator. While this approach enabled us to obtain simulated results very close to the ones obtained experimentally, ideally the material properties of the elements of the system should be disclosed by the manufactures in order to facilitate comparisons between solutions that didn't involve time consuming experimental procedures.

8. BIBLIOGRAPHY

[1] Govind P. Agrawal, *Fiber-Optic Communication Systems*, 3rd ed. John Wiley & Sons, Inc., 2002.

[2] G. J. Holzmann and B. Pehrson, *The Early History of Data Networks*. IEEE Computer Society Press, 1995.

[3] T. H. Maiman, “Stimulated Optical Radiation in Ruby,” *Nature*, vol. 187, no. 4736, pp. 493–494, 1960.

[4] R. N. Hall, G. E. Fenner, J. D. Kingsley, T. J. Soltys, and R. O. Carlson, “Coherent light emission from GaAs junctions,” *Phys. Rev. Lett.*, vol. 9, no. 9, pp. 366–368, 1962.

[5] J. Hecht, “The Birth of the Diode Laser,” *Opt. Photonics News*, vol. 18, no. August, pp. 38–43, 2007.

[6] D. F. Welch and S. Member, “A Brief History of High-Power Semiconductor Lasers,” *IEEE J. Sel. Top. QUANTUM Electron.*, vol. 6, no. 6, pp. 1470–1477, 2000.

[7] V. C. Coffey, “Sea Challenge: The Challenges Facing Submarine Optical Communications,” *Opt. PHOTONICS NEWS*, no. March, 2014.

[8] C. S. I. Cisco, *Cisco Visual Networking Index: Forecast and Methodology, 2015–2020*. 2016.

[9] R. Enright, K. Nolan, I. Mathews, A. Shen, G. Levaufre, R. Frizzell, and D. Hernon, “A Vision for Thermally Integrated Photonics Systems,” *Bell Labs Tech. J.*, vol. 19, pp. 31–45, 2014.

[10] R. S. Tucker, *Green Optical Communications — Part I : Energy Limitations in Transport*, vol. 17, no. 2. IEEE Computer Society Press, 2011.

[11] R. S. Tucker, *Green Optical Communications — Part II : Energy Limitations in Networks*, vol. 17, no. 2. IEEE Computer Society Press, 2011.

[12] Broadband Forum, *MR-204 Energy Efficiency, Dematerialization And The Role Of The Broadband Forum*, no. 1. BroadbandSuite Solutions Series – Green, 2009.

[13] O. P. Inc., “Optima Laser Diode Application Notes and Glossary.” [Online]. Available: http://www.optima-optics.com.

[14] M. Ettenberg, “Specifications and characteristics of laser diodes for the user,” 1986.

[15] P. E. Phelan, T. T. Lee, V. Chiriac, E. E. Road, and M. D. El, *Current and future miniature refrigeration cooling technologies for high power microelectronics*. IEEE Computer Society Press, 2003.

[16] J. Gao, X. Han, and Y. Yu, “Thermal characteristics simulation of semiconductor lasers packaging for high speed application,” *16th Int. Conf. Electron. Packag. Technol. ICEPT 2015*, no. 11174097, pp. 8–11, 2015.

[17] I. Weir, G. Archenhold, M. Robinson, M. Williams, and P. Hilton, “Photonics Technologies and Markets for a Low Carbon Economy,” 2012.

[18] T. J. Seebeck, “Ueber die magnetische Polarisation der Metalle und Erze durch TemperaturDifferenz,” *Ann. Phys.*, vol. 82, no. 2, pp. 133–160, 1826.

[19] J. Peltier, “Nouvelles Experiences sur la Caloriecete des Courans Electrique,” 1834.

[20] A. G. Mikerov, “From history of electrical engineering III: Electromagnetism discovery and its fundamental laws in the first half of 19-th century,” *Proc. 2014 IEEE North West Russ. Young Res. Electr. Electron. Eng. Conf. ElConRusNW 2014*, pp. 1–7, 2014.

[21] W. Thomson, “On a mechanical theory of thermoelectric currents,” *Proc. R. Soc. Edinburgh*, pp. 91–98, 1851.

[22] E. K. Vedernikov, M.V.; Iordanishvili, “A . F . Ioffe and Origin of Modern Semiconductor Thermoelectric Energy Conversion,” *17th Int. Conf. Thermoelectr.*, vol. 1, no. 1 998, pp. 37–42, 1998.

[23] R. E. Simons, R. C. Chu, and I. B. Machines, *Thermoelectric Cooling to Electronic Equipment: A Review and Analysis*. IEEE Conference Publications, 2000.

[24] D. S. Alles, “Trends in Laser Packaging,” *Proc. 40th ECTC*, pp. 185–192, 1990.

[25] M. Csele, *Fundamentals Of Light Sources And Lasers*. John Wiley & Sons, Inc., 2004.

[26] W. T. Silfvast, “Fundamentals of Photonics -Lasers,” *Cochrane Database Syst. Rev.*, vol. 5, pp. 1–44, 2003.

[27] R. N. Abed, “the Thermal Management System of Laser Diode : a Review,” *ARPN J. Eng. Appl. Sci.*, vol. 10, no. 12, pp. 5250–5260, 2015.

[28] P. a. Kirkby, “Semiconductor laser sources for optical communication,” *Radio Electron. Eng.*, vol. 19, no. 7–8, p. L621, 1981.

[29] H. Kressel and J. K. Butler, “Semiconductor Lasers and Herterojunction Leds,” *Semicond. Lasers Herterojunction Leds*, pp. 77–116, 1977.

[30] Agilent Technologies, “Measuring Extinction Ratio of Optical Transmitters Application Note 1550-8,” *Agil. Technol. - Innov. HP W.*, pp. 1–31, 2001.

[31] J. M. Senior and M. Y. Jamro, *Optical Fiber Communications: Principles and Practice*. FT Prentice Hall, 2009.

[32] H. S. Lee, *Thermal Design: Heat Sinks, Thermoelectrics, Heat Pipes, Compact Heat Exchangers, and Solar Cells*, vol. 53, no. 9. John Wiley & Sons, Inc., Hoboken, New Jersey, 2010.

[33] H. Lee, “The Thomson effect and the ideal equation on thermoelectric coolers,” *Energy*, vol. 56, pp. 61–69, 2013.

[34] S. Lwe and L. Weera, “Analytical Performance Evaluation of Thermoelectric Modules Using Effective Material Properties,” 2014.

[35] H. Lee, A. M. Attar, and S. L. Weera, “Performance Prediction of Commercial Thermoelectric Cooler Modules using the Effective Material Properties,” *J. Electron. Mater.*, vol. 44, no. 6, pp. 2157–2165, 2015.

[36] M. J. Huang, R. H. Yen, and A. B. Wang, “The influence of the Thomson effect on the performance of a thermoelectric cooler,” *Int. J. Heat Mass Transf.*, vol. 48, no. 2, pp. 413–418, 2005.

[37] C. Y. Du and C. Da Wen, “Experimental investigation and numerical analysis for one-stage thermoelectric cooler considering Thomson effect,” *Int. J. Heat Mass Transf.*, vol. 54, no. 23–24, pp. 4875–4884, 2011.

[38] MITSUBISHI (OPTICAL DEVICES), “1.55 um DFB-LD Module With Singlemode Fiber Pigtail,” *FU-68SDF-V802MxxB datasheet*. [Online]. Available: http://www.datasheetcatalog.com/.

[39] L. FURUKAWA ELECTRIC CO., “1480nm Laser Diode Module with FBG,” *OD-KCB3001 datasheet*, 2011. .